



Contents lists available at ScienceDirect

Progress in Quantum Electronics

journal homepage: www.elsevier.com/locate/pqe

Review

Laser ignition - Spark plug development and application in reciprocating engines



Nicolai Pavel^{a,*}, Mark Bärwinkel^b, Peter Heinz^b, Dieter Brüggemann^b,
Geoff Dearden^c, Gabriela Croitoru^a, Oana Valeria Grigore^a

^a National Institute for Laser, Plasma and Radiation Physics, Laboratory of Solid-State Quantum Electronics, Atomistilor 409, Magurele 077125, Ilfov, Romania

^b University of Bayreuth, Department of Engineering Thermodynamics and Transport Processes, Universitätsstraße 30, 95447 Bayreuth, Germany

^c University of Liverpool, School of Engineering, Liverpool L69 3HG, UK

ARTICLE INFO

Keywords:

Diode-pumped solid-state lasers
Passively Q-switched laser
Laser ignition of engines
Lean-fuel ignition
Laser induced combustion
Flame kernel

ABSTRACT

Combustion is one of the most dominant energy conversion processes used in all areas of human life, but global concerns over exhaust gas pollution and greenhouse gas emission have stimulated further development of the process. Lean combustion and exhaust gas recirculation are approaches to improve the efficiency and to reduce pollutant emissions; however, such measures impede reliable ignition when applied to conventional ignition systems. Therefore, alternative ignition systems are a focus of scientific research. Amongst others, laser induced ignition seems an attractive method to improve the combustion process.

In comparison with conventional ignition by electric spark plugs, laser ignition offers a number of potential benefits. Those most often discussed are: no quenching of the combustion flame kernel; the ability to deliver (laser) energy to any location of interest in the combustion chamber; the possibility of delivering the beam simultaneously to different positions, and the temporal control of ignition. If these advantages can be exploited in practice, the engine efficiency may be improved and reliable operation at lean air-fuel mixtures can be achieved, making feasible savings in fuel consumption and reduction in emission of exhaust gasses. Therefore, laser ignition can enable important new approaches to address global concerns about the environmental impact of continued use of reciprocating engines in vehicles and power plants, with the aim of diminishing pollutant levels in the atmosphere. The technology can also support increased use of electrification in powered transport, through its application to ignition of hybrid (electric-gas) engines, and the efficient combustion of advanced fuels.

In this work, we review the progress made over the last years in laser ignition research, in particular that aimed towards realizing laser sources (or laser spark plugs) with dimensions and properties suitable for operating directly on an engine. The main envisaged solutions for positioning of the laser spark plug, i.e. placing it apart from or directly on the engine, are introduced. The path taken from the first solution proposed, to build a compact laser suitable for ignition, to the practical realization of a laser spark plug is described. Results obtained by ignition of automobile test engines, with laser devices that resemble classical spark plugs, are specifically discussed. It is emphasized that technological advances have brought this method of laser ignition close to the application and installation in automobiles powered by gasoline engines. Achievements made in the laser ignition of natural gas engines are outlined, as well as the utilization of

* Corresponding author.

E-mail addresses: nicolaie.pavel@infpr.ro (N. Pavel), lttt@uni-bayreuth.de (M. Bärwinkel), g.dearden@liverpool.ac.uk (G. Dearden).

<http://dx.doi.org/10.1016/j.pquantelec.2018.04.001>

Available online 13 April 2018

0079-6727/© 2018 The Author(s). Published by Elsevier Ltd. This is an open access article under the CC BY-NC-ND license (<http://creativecommons.org/licenses/by-nc-nd/4.0/>).

laser ignition in other applications. Scientific and technical advances have allowed realization of laser devices with multiple (up to four) beam outputs, but many other important aspects (such as integration, thermal endurance or vibration strength) are still to be solved. Recent results of multi-beam ignition of a single-cylinder engine in a test bench set-up are encouraging and have led to increased research interest in this direction.

A fundamental understanding of the processes involved in laser ignition is crucial in order to exploit the technology's full potential. Therefore, several measurement techniques, primarily optical types, used to characterize the laser ignition process are reviewed in this work.

1. Introduction

Vehicles powered by internal combustion engines are still predominantly applied, but human concerns about environment impact of the ongoing use have grown meanwhile. They triggered and intensified further investigations in various related research subjects of this field. The prevailing development for future engines focussed on combustion systems that can burn different fuels, but are moreover capable of addressing several critical requests, such as fuel economy or decreased emission of exhaust gases without reducing the engine efficiency or power. Since the early 20th century, high-voltage spark plugs are predominantly applied to initiate combustion in a fixed location and at a certain moment within each engine cycle. Constant improvements have made the electrical spark plug more effective and reliable, still being a simple and inexpensive ignition device. On the other hand, an electrical spark plug has reduced capability in igniting diluted air-fuel mixtures and presents limited performance under high-pressure conditions. Furthermore, the spark position is determined by the cylinder geometry, resulting in inflexibility of the ignition spot position inside the combustion chamber. Electric spark plug electrodes suffer from wetting and erosion, and their protrusion into the cylinder volume can quench the kernel of the emerging flame during combustion.

Lasers are attractive ignition sources as proven by extensive research in the field of laser ignition (LI) performed in the last few decades. In competing with electric spark plug ignition LI offers several advantages, at least theoretically. First, there is no quenching effect of the combustion flame kernel. This is because a laser beam can be transferred to and subsequently focussed into an engine cylinder by a few optical elements (in general these are some lenses and a window) that are placed externally to the cylinder. The internal protruding electrodes of an electrical spark plug are redundant. Another major advantage of LI is the ability to target the laser beam to any benefiting point within the combustion chamber. In this way the flame propagation distance can be optimized and the combustion duration can be reduced. Furthermore, LI offers the possibility to deliver the beam simultaneously to different spots, realizing the so-called 'spatial multipoint ignition' (i.e. the spatial control of LI). Additionally, a train of laser pulses can be aimed at the same spot within a very short time span, achieving multiple-pulse ignition or the temporal control of LI. Namely these two last features could offer ignition devices for reciprocating engines of lean air-fuel mixtures or high-pressure mixtures, although they are not easy to be exploited.

Considering all these advantages, LI has been investigated in stationary gas engines for energy cogeneration, in ground-based turbines, aero turbines and rocket engines, in scramjet engine or in reciprocating engines. Up to now there seems to be no commercial combustion engine that is driven by such an LI system, or at least that was operated with LI for a long time period (comparable with the lifetime of an electrical spark plug). Only recently, i.e. after 2012–2013, automobiles with gasoline engines were entirely run with laser sparks by two research groups (details to be given later).

The purpose of this work is to review the research done on LI of internal combustion engines, especially on gasoline engines. A short history of LI development will be presented in section 2. Section 3 is dedicated to the steps taken to develop a spark-plug-like laser system and its application in LI of automobile engines. Several approaches for delivering the laser radiation inside of the engine cylinder, like a) transporting the beam through a fiber from a remote laser or b) positioning the laser spark plug on the engine similar to a traditional spark plug, are discussed. The pump of a laser spark with conventional diode laser or further use of Vertical Cavity Surface Emitting Laser (VCSEL) as pump source is considered. Multi-point LI and its advantages on the ignition of an engine are reviewed. Following many years of research the achievement obtained in Japan, where the first car was run only by laser sparks, is noted. The results obtained at the National Institute for Laser, Plasma and Radiation Physics (INFLPR), Magurele, Romania in the field of LI of an automobile engine will be discussed. Several results obtained by LI of natural gas reciprocating engines are mentioned. To take full advantage of LI of an engine, a basic understanding of the LI process is necessary. Therefore, an overview of optical measurement techniques to investigate and to characterize the LI process is given in section 4. Results obtained by the research group from Bayreuth University, Germany regarding the characteristics of LI are discussed in this section, but also the work of other research groups is referenced. Section 5 concludes this work.

2. "History" of laser ignition

It is generally recognized that the first demonstration of laser-induced optical breakdown phenomenon in air [1] can be considered as the starting point for research on LI. In this experiment, a frequency-tripled Q-switched ruby laser pulse was focused by a lens and generated plasma, comparable to an electrical discharge between the electrodes of a spark plug. Probably due to the experimental complexity, the authors described their set-up as "the most expensive spark plug in automotive industry".

Soon after, the ignition of chemically reactive gaseous mixtures in a combustion chamber (or 'explosion bomb') was investigated by

Lee and Knystautas in 1969 [2]. Using a ruby laser, Q-switched by a rotating roof prism and saturable absorber (SA) dye cell, and yielding single 10 ns duration pulses, the minimum energy required to induce breakdown was found to be 1.2 J. The ignition mechanisms were discussed, showing a strong connection to the dynamics of the decaying blast for both detonable and non-detonable mixtures.

Results regarding the minimum ignition energy (MIE) for stoichiometric methane-air mixtures were reported by Weinberg and Wilson in 1971 [3], by employing a passively Q-switched ruby laser (30 J energy per pulse, 20 ns duration). It was pointed out that ignition by laser could initiate plasma in shorter times and smaller volumes compared to electric spark discharges. In addition, for the case of LI there were no energy losses induced by the presence of spark plug electrodes. The influence of the laser pulse duration and the methane-air pressure on the blast wave was investigated. It was observed that LI is able to provide several benefits (such as decreased MIEs and quenching distances) for low pressure of methane-air mixture and it was suggested that shorter laser pulses are needed in the case of high pressure where plasma of small size is desirable. Interest in LI was shown by General Motors Corp. with the paper published in 1974 by Hickling and Smith [4]. Here, ignition of fuels including isooctane, cyclohexane, *n*-heptane, *n*-hexane, clear indolene and diesel was investigated in a combustion bomb. Interestingly, the authors considered LI to be impractical “because of its low efficiency and high cost,” yet highlighted some possible advantages in comparison with a standard spark plug, pointing out that “the laser spark is electrodeless and can be positioned anywhere inside the combustion chamber”.

The first use of a laser beam as an ignition source for an internal combustion engine (and that was ignited at the optimum moment) was described by Dale et al., in 1978 [5,6]. There, a one-cylinder engine (ASTM-CFR) allowed operation with air-fuel (A/F) ratio between 12:1 and the lean limit. It was fitted with a zinc selenide window, through which a beam delivered by a CO₂ laser (pulses of 0.3 J energy and 50 ns duration at 10.6 μm wavelength) was focused by a set of lenses to different positions inside the chamber. Various measurements were made for both LI and ignition by classical spark; these included the in-cylinder pressure, the specific fuel consumption, the engine power generated and the exhaust gas emissions. It was found that LI improved the engine performance and efficiency. In addition, an extension of the lean limit of operation, up to A/F = 22.5, was observed for LI. No notable differences between CO and HC emissions were found. However, an increase of NO_x emission was measured for the case of LI and attributed to the higher temperatures reached in the cylinder due to more rapid combustion. It was noted that, for both LI and classic ignition cases, adding Exhaust Gas Recirculation (EGR) reduced the NO_x at all A/F ratios used in the experiments. A further significant finding related to the spark location was that the engine performance was found to be improved by moving the LI focus away from the cylinder walls.

Many investigations on the characteristics of combustion obtained by LI were performed later. A review and comparison of the initiation of combustion processes by conventional electrical sparks and with laser were published by Ronney in 1994 [7]. In this work, the main advantages of LI were considered to be the free choices of both position and timing of the laser-induced spark. The energy requirements were believed not to be substantially different to those of conventional ignition. Moreover, reducing the burning time in the case of LI was considered to demonstrate a possibility to burn quickly and expand the product gases at low temperatures, which would minimize the amount of NO_x produced.

Various characteristics of combustion of methane-air mixtures were analyzed by Ma et al. [8] in a four-stroke (Otto-cycle) single-cylinder combustion chamber, using different lasers: namely, a krypton fluoride (KrF) gas excimer laser at 248 nm, an argon fluoride (ArF) gas excimer laser at 193 nm and a Nd:YAG laser at 1064 nm. No significant difference in ignition time delay was found between each of these three laser sources. Furthermore, a lower cylinder pressure was measured for ignition by the ArF laser, compared with pressures measured when applying the KrF and Nd:YAG lasers. In addition, within the same chamber and under the same ignition conditions, the time taken for combustion to reach the peak pressure was shorter (by 4–6 ms) for LI compared with the classic ignition. The laser-induced breakdown and propagation of the expansion wave were examined. For a methane-air equivalence ratio $\Phi = 1$, ignition by electric spark failed, while LI remained reliable and the cycle-to-cycle variation of pressure was improved in comparison with electrical spark ignition.

Ignition of methane-air mixtures was also investigated by Phuoc and White [9] employing a ns-pulse Q-switched Nd:YAG laser at 1064 nm. Laser irradiances of 10^{12} – 10^{13} W/cm² were used to ignite methane-air mixtures with equivalent ratio (ER) ranging from 0.66 (6.5% methane) to 1.95 (17% methane). Variations in the threshold laser energy could be explained by electron-cascade theory (i.e. the electron-ion inverse bremsstrahlung process). The MIE increased either side of stoichiometry, for both increasingly lean and increasingly rich mixtures. The MIE also increased by around an order of magnitude for LI compared with electrical spark plug ignition. It was concluded that LI did not work well at lean conditions, but was favorable for ignition of fuel-rich mixtures.

A ns-pulse Nd:YAG laser at 532 nm was employed to determine the MIE of several fuel-air mixtures including propane, dodecane and jet-A fuel [10]. The minimum energy for LI of the propane-air mixture at atmospheric as well as at lower pressures was larger than corresponding results obtained using electrical spark ignition. A larger optimum equivalent ratio was determined for heavier hydrocarbon fuels concerning the MIE. The jet-A fuel exhibited a parabolic variation of the MIE because the temperature and pressure conditions cause a shift in the air-fuel ratio (AFR) from lean to rich. Furthermore, a decrease in jet-A fuel loading is accompanied by an increase in the MIE whereas the pressure dependence on the MIE is less observable when fuel is changed from propane to dodecane and to jet-A fuel.

The MIE necessary to ignite a laminar premixed methane-air mixture was determined using a ns-pulse Q-switched Nd:YAG laser at 532 nm and high-speed Schlieren imaging [11]. The important influence of the flow instabilities generated by the temperature gradient around the flame kernel was noted. The evolution of MIE for lean and rich equivalence ratios was investigated. A research group from Vienna University, led by Wintner E., has studied ignition of methane-air mixtures at high pressure with a ns-pulse Nd:YAG laser operating at 1064 nm, 532 nm and 355 nm [12]. It was concluded that an optimized Gaussian laser beam can reduce the MIE necessary for LI, reaching a level where conventional ignition sources can be reasonably replaced by lasers. MIE decreased down to 8 mJ at pressures up to 4 MPa and a laser beam that was focussed to a spot of about 20 μm in diameter. Lean methane-air mixtures (air-fuel

equivalence ratio, λ of 0.56) were successfully ignited with a slight increase of the laser pulse energy above this value. Wavelength dependence of MIE was not observed; this finding supported the idea that laser plasma generation is initiated from the interaction of the laser beam with small particle impurities.

Ignition of ultra-lean methane/hydrogen/air mixtures at high temperature and pressure [13] and of hydrogen-air mixtures at high pressure [14] was characterized by the same research group with a ns-pulse Q-switched Nd:YAG laser at 1064 nm. Engine like conditions in constant volume chamber were considered in the experiments. Hydrogen was added to improve the combustion characteristics at the lean limit ($\lambda = 1.9$) of methane-air mixtures [13]. Moreover, the multi-point ignition was adopted to accelerate the combustion. For the two-point LI of hydrogen-air mixtures with an air-fuel equivalent ratio of $\lambda = 4$, the time to reach the peak pressure was reduced by 50% for the ignition in two points in comparison with one-point LI. Higher peak pressures by about 7% were measured. An influence of a three-point ignition on these parameters was not detectable. In addition, the MIE for ignition was found to decrease with higher initial pressures [14]. This finding was in contrast to ignition by an electrical spark plug, where a rise in the initial pressure led to an increase in the MIE. It was also argued that positioning of the plasma in the center of the combustion chamber decreases the total combustion time.

In contrast to the studies mentioned above, laser-induced spark generation in air was experimentally investigated and theoretically analyzed by Phuoc [15]. Blast-wave theory was used to determine the shock radius R , which was found to vary proportionally with time t following a $t^{2/5}$ law. Furthermore, the shock pressure was found to vary as R^{-3} , and 70% of the spark energy was determined to be used up in the shockwave development. For low spark energies the radiation energy loss was found to be 22%; this loss becomes comparable to that due to the shock expansion when high spark energies were used.

All these works demonstrate that LI has developed to become a very interesting and active research topic. Many other papers can be cited to support this statement. Fundamental aspects and applications of LI can be found in the review articles published by Bradley et al. [16] and Phuoc [17]. Regarding the latter, it is worthwhile mentioning several conclusions drawn. It was stated that many features of a laser beam (such as multipoint ignition, possibility to move the ignition point, or multiple pulse ignition) were not fully exploited in the studies on lean fuels. Based on this, the improvements expected from LI will not be obtained easily just by replacing the electrical spark plug with a laser. In addition, the possibility of adjusting the ignition point indicates that LI could be more suitable for jet engines and gas turbine engines (i.e. for lean premixed combustion engines). Moreover, it was pointed out that the high costs of an LI system could be a significant impediment for practical applications.

More recently, a comparative study of LI and ignition by classical spark plug in gasoline-air mixtures was reported by Xu et al. [18]. Q-switched Nd:YAG laser pulses (with duration of 7.9 ns at 1064 nm and 6.6 ns at 532 nm) were used to evaluate the ignition probability and to determine MIE. In their experiments, differences were observed in the MIE for LI when using two different laser wavelengths. Specifically, for an AFR = 1, the MIE was found to be 13.5 mJ for ignition at 1064 nm, and 9.5 mJ for ignition at 532 nm. An extension of the lean flammability limit by LI from 0.8 to 0.6 was also noted.

One important step toward the use of LI in automotive applications was made at Technical University Vienna (TUW), by the use of a Q-switched Nd:YAG laser (at 1064 nm) to ignite a single-cylinder research engine [19]. It was concluded that LI reduces the fuel consumption by several percent in comparison with ignition by the electrical spark plug. A decrease of the exhaust emissions by about 20% was noted. LI was also performed with a frequency-doubled Nd:YAG laser at 532 nm and no differences were found in comparison with the data obtained with the first-mentioned laser source. Furthermore, the operation of the engine for 20 h was performed in order to study the influence of deposits caused by the combustion process on the entrance window. The cold start of the engine was also successfully realized. It was observed that above of a certain intensity of the laser beam at the entrance window the engine can operate without misfiring. The advantage of LI in enabling flexibility of choice of the ignition location inside the cylinder was emphasized.

A single cylinder research engine was ignited by Alger et al. [20] with a flash-lamp pumped Nd:YAG laser (pulses at 1064 nm with 50 mJ energy and 6 ns duration). The lean limit was determined with LI for premixed iso-butane and propane fuels. The energy density influence on the ignition kernel was also investigated. At a fixed focal volume there is a threshold of ignition beyond little benefit is obtained by increasing the energy density. Furthermore, the lean performances are decreased when energy density is increased by reducing the dimension of the focal volume beyond a certain value. It was concluded that LI can ignite mixtures with equivalent ratio much lower than that typically obtained for classical spark ignition, yet still having acceptable combustion stability - a Coefficient of Variance in Indicated Mean Pressure (COV_{IMEP}) of less than 5% was reported for propane with $\lambda = 0.45$.

At the University of Liverpool, a Q-switched Nd:YAG laser (1064 nm) was employed to ignite one cylinder of a 4-cylinder Ford Zetec port fuel injection (PFI) petrol test engine [21]. The ability to vary the laser pulse energy and duration (5–20 mJ and 6–15 ns, respectively) enabled a study of the influence of these laser parameters on the engine performance. The engine was run at 1200, 2000 and 4000 rpm. Laser pulse energies between 7 mJ and 8 mJ, focused to beam waists between 65 μm and 85 μm in diameter were shown to give successful combustion without misfires and without inducing damage to the optics. The stability of the engine was determined in terms of Coefficient of Variance (COV), both in COV_{IMEP} and Peak Cylinder Pressure Position (Var_{PPP}). Thus, through optimization of the laser beam parameters, the engine could run with LI for several hours, showing stability in COV_{IMEP} and COV_{PPP} equivalent to values measured for ignition by the conventional spark plug. A focal distance of 4 mm from the cylinder wall was found to be optimum for LI, similar to the position of the electrical spark plug originally used for the engine. In later experiments, the same research group succeeded for the first time in operating the 4-cylinder test engine entirely by LI [22]. In these experiments, the beams of two Q-switched Nd:YAG lasers (1064 nm) were electro-optically switched between 4 engine cylinders, and directed to and focused into each of them by equivalent optics (lenses and mirrors). The engine was operated over a large range of speeds (800–2400 rpm), loads (50–75 N m) and various ignition timings (16° to 36° before top dead center). The measurements concluded that LI improved the combustion stability, in terms of COV_{IMEP} and Var_{PPP} , in comparison to ignition by an electrical spark. A key finding of this work was that much leaner air-fuel mixtures could be ignited by LI compared to spark plug, and with reduced cyclic variation.

Other essential aspects about LI can be found in the review papers published by Tauer et al., in 2010 [23] and Morsy in 2012 [24].

We can conclude at this point that even further developments in laser technology are required. There is a recognized need for compact laser sources, robust enough to work reliably in adverse conditions of pressure, vibration and temperature and that could be installed directly on an engine, similar to classical spark plugs.

3. Laser spark plug development and application in laser ignition

3.1. Fiber delivery for laser ignition application

The results mentioned in Section 2 were obtained with combustion chambers (open chambers or single cylinders); a transparent window was used to insert the laser beam inside the chamber and focusing was done with lenses. The beams were delivered by commercial lasers that were positioned nearby the engine. Still, although not yet practical, such an experimental set-up can be improved. One solution investigated for transferring the laser pulse from the source to the engine is by use of an optical fiber. The flexibility of a fiber allows a free transfer path, with less influence of vibrations on optical alignment. It is also not prone to dirt and pollution and requires small space necessary for mounting. In addition, the beam exiting the fiber end can be relatively easily focused into the combustion chamber.

A variety of optical fibers, like step-index fibers with diameters between 100 μm and 1000 μm , hollow-core dielectric capillarity fibers, hollow glass fibers with cyclic olefin polymer-coated silver and hollow-core photonic crystal fibers were tested by Stakhiv et al. [25]. It was concluded that only the hollow-core photonic crystal fibers could be a candidate for practical use in LI.

The first delivery of ns-laser pulses through flexible fibers and generation of optical sparks in gasses at atmospheric pressure was reported by Yalin et al. [26]. The light source was a Q-switched Nd:YAG laser at 1064 nm with 8 ns pulse duration at 5 Hz repetition rate and good beam quality (laser beam $M^2 < 2$). The beam was launched in a cyclic olefin polymer-coated silver hollow fiber with an inner diameter of 700 μm and a length of 1 m. The transmitted beam presented a high optical intensity (about 2 GW/cm^2) and good divergence (~ 0.01 rad half angle) when the coupling into the fiber was made at a low angle (~ 0.01 rad half angle). In these conditions, nearly 70% of the input laser energy of 47 mJ was transmitted through the fiber. This allowed focusing of the transmitted laser beam to high intensity, enough to generate sparks. The effect of fiber bending on the characteristics of the transmitted laser beam was also investigated. A decrease of the transmission was measured when bending curvature was increased, which in turn led to reduced optical intensity of the focused beam and lower probability for creating optical sparks.

A hollow core photonic crystal fiber (PCF) with a diameter of 15 μm was used by Al-Janabi to transport the laser beam of a Q-switched Nd:YAG laser at 1064 nm, with 5.5 ns pulse duration and quality $M^2 \sim 1.8$ [27]. The fiber was contained inside a vacuum chamber to avoid breakdown in the air that fills the fiber. Methane-air mixtures were ignited with laser pulses of only 150 μJ that were focused with an aspherical lens to a diameter of about 4 μm .

An extensive analysis of various types of fibers aiming the delivery of laser beams with the high intensity required for spark formation was made by Joshi et al. [28]. Olefin polymer coated hollow core fibers 2 m in length with core diameter of 1 mm, considered reasonable for a practical LI system, were employed in the experiments. A Q-switched Nd:YAG laser (1064 nm wavelength) with 8 ns pulse duration at 10 Hz repetition rate and beam quality $M^2 < 2$ was the laser source. It was found out that the launch conditions of the laser beam into the hollow fiber has a significant influence on mode coupling, the transmission and the quality of the transmitted beam. The effect of fiber bending on the fiber transmission performances was also investigated. In a separate experiment, laser breakdown in air was obtained with pulses of 2.4 mJ energy and 0.7 ns duration (i.e. 3.4 MW peak power) yielded by an 80 μm core fiber laser amplifier. This was the first demonstration that fiber lasers can be used to realize optical sparks. It was also concluded that solid-core fibers are not suitable for the transport of beams that can induce spark at atmospheric conditions. Still, the use of such fibers was feasible with a reduction in the output numerical aperture (NA) and at high pressure conditions. Later, El-Rabii and Gaborel demonstrated LI of *n*-heptane/air and JP4/air mixtures via a solid core optical fiber [29]. Beam delivery of a Q-switched Nd:YAG laser (at 1064 nm, ns duration pulses) was achieved through optical fibers of 150 cm length and with various diameters (between 200 μm and 940 μm). Laser pulses with maximum energy of 45 mJ were transmitted through a fiber with a diameter of 940 μm . No sparking was recorded in the air at atmospheric pressure. Nevertheless, the transmitted pulses could be focused sufficiently to ignite in similar conditions the fuel-air mixtures used in the experiments. Moreover, sparks in the air were produced at pressures above 4 bar. It was pointed out that critical parameters for LI are the coupling conditions and the fiber curvature.

The group from the University of Liverpool has also investigated the possibility to use optical fibers in a laser-induced ignition system by delivering high-power laser beams to an optical plug [30]. Multi-mode step-index silica fibers, sapphire fibers, large mode area PCFs and multi-mode PCFs with ultra-high NA, all with a length of 1 m and having various core sizes (ranging between 35 μm and 600 μm) and NA (0.046–0.64) were used in the experiments. The testing was done with a flash-lamped pumped, Q-switched Nd:YAG laser at 1064 nm delivering pulses with 15 ns duration. Investigations were performed on a Ford Zetec IC test engine with the fiber optical plug mounted in one cylinder; the other cylinders were operated by electrical spark plugs. The use of free standing fiber ends, in the case of step-index silica fiber, increases the damage threshold to 9 GW/cm^2 from the ~ 3 GW/cm^2 threshold measured when fixing of fibers with adhesive in SMA connectors. The damage thresholds for both PCFs were measured to be ~ 7 GW/cm^2 . The sapphire fibers presented the lowest damage threshold of ~ 4 GW/cm^2 . The influence of fiber bending on the output beam intensity profile and optical losses was studied. It was also found that engine vibrations and engine speed has an influence on the divergence of the transmitted laser beam, effects that are not desirable for an LI system with fiber-delivery. Step-index silica fibers with diameters of 400 μm and 600 μm and NA of 0.12 and 0.22 were tested on the engine. The percentage of LI combustion events was around 35% for the 600 μm diameter fiber (65 mJ transmitted energy) and only 8% for the 400 μm diameter fiber (50 mJ transmitted energy). These results were not considered reliable, but further online tests gave data that were considered encouraging for achieving 100% combustion percentage with a fiber beam

delivery system. Bundling or multiplexing were solutions proposed for increasing the damage threshold when using other fiber types, such as hollow core photonic band-gap fibers, not used in this study.

The first demonstration of delivery of ns laser pulses with solid core silica fibers and realization of sparks in the air at atmospheric pressure with 100% probability was reported by Joshi et al., in 2012 [31]. A Q-switched Nd:YAG laser (1064 nm wavelength, 9.5 ns pulse duration, $M^2 < 2$) was used in the experiments. Fibers with clad-to-core diameter ratios much larger than 1.1 (400 μm core diameter and 720 μm diameter clad) and lengths of 1.8–2.0 m were tested. Reliable sparking (100% probability) was obtained at atmospheric pressure with 3.1 mJ laser pulse energy exiting the fiber and focused to a diameter of 8 μm (i.e. 420 GW/cm² intensities). Furthermore, testing on a single-cylinder gas engine (a Waukesha co-operative fuel research engine that ran on bottled methane) was performed. A laser beam with 11 mJ pulse energy at 25 ns duration was delivered to the optical spark plug with a clad fiber of 2.85 m in length, the core diameter of 400 μm and 720 μm clad diameter. It was found that 7 mJ of pulse energy was transmitted and focused into the cylinder. The engine was operated within its ignition limits of air-methane ratio and boosts, showing reliable spark formation and engine ignition (on 100% of the laser shots).

A review paper on high-power fiber delivery research for LI applications was published in 2013 by Yalin [32]. It was pointed out that such methods for beam delivery and realization of combustion initiating sparks still faces numerous technical challenges. Results obtained with coated hollow fibers, step-index silica fibers, large-clad fibers, photonic crystal fibers and Kagome fibers were described and analyzed. Multiplexed fibers can reduce the amount of lasers necessary for ignition of an engine and therefore were considered of interest in future. Information regarding optical fiber delivery for LI can be found in the article also published in 2013 by Dearden and Shenton [33]. It was underlined that particularly promising for LI are Kagome fibers [32] and hollow-core optical fibers [33]. The paper published in 2014 by Dumitrache et al. [34] supported these statements. A Kagome fiber with hypocycloid-shape internal structure, having 50 μm core diameter, was used to transport pulses yielded by a 1064 nm Q-switched Nd:YAG laser with energy up to 30 mJ at 30 ns duration. The energy deliverable through the fiber was increased (from 5 mJ to 30 mJ) by lengthening the pulse duration (from 7 ns to 30 ns), while the safety operation margins were also improved. Very importantly, LI of a single-cylinder Ford engine with gasoline direct injection (GDI) was demonstrated with such a fiber-delivery system. Reliability (100% probability) was achieved at 2400 rpm engine speed for short (maximum few hours) duration tests.

3.2. Compact solid-state lasers for laser ignition. Diode-laser pumping

The possibility to deliver a laser beam from the laser source to the engine is very attractive, but still the issues associated with the laser used in the experiments (in principal large size and heavy weight, or low output efficiency) and that it should be located in a car requires a solution. Therefore, it was clear that research should focus on developing compact lasers, able to deliver pulses with high-peak power and to be mounted on the car, preferably directly on the engine, just as a traditional spark plug.

The concept for a laser spark plug was described by Weinrotter et al., in 2005 [35]. The solution for “noncentral ignition source” with one ignition laser on each cylinder of an engine and a pump source located apart was preferred. Thus, in order to simplify the laser system by avoiding high voltage required in electro-optically Q-switched lasers it was stated that the laser (a microchip laser) has to be passively Q-switched. Furthermore, building the device in a monolithic structure will lead to a robust system, which can also facilitate mass production. It was also outlined that the optical pumping has to be made in quasi-continuous wave (quasi-cw) with diode lasers, and optical fibers can be used to transfer the pump beam (that has low peak power) from a diode to the corresponding laser spark plug. A sketch of an engine on which such a miniature solid-state is mounted can be seen in Fig. 1 [35,36].

The demonstration of such a laser was made in 2007 by Kofler et al. [37]. The solution was a solid-state Nd:YAG active medium, passively Q-switched by a Cr⁴⁺:YAG SA. The Nd:YAG was optically pumped at 808 nm by a fiber-coupled diode laser operated in quasi-cw mode. Maximum pump power delivered was 300 W at 500 μs pump pulse duration. An important feature was the longitudinal

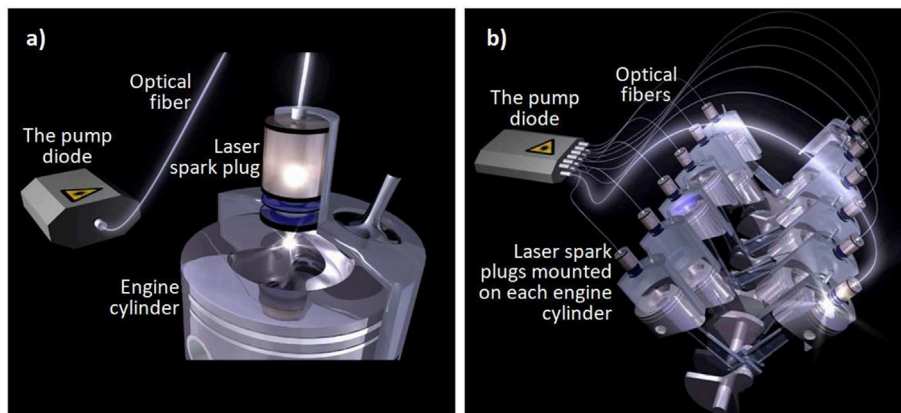


Fig. 1. Computer illustration of an end-pumped by fiber-coupled diode lasers, passively Q-switched solid-state laser with pump diode positioned apart from the engine and the laser head mounted directly a) On the engine cylinder [35] and b) On a 12-cylinder internal combustion engine [36].

pumping (or end pumping) of the Nd:YAG crystal. A study aimed at optimization of such a laser, including the output coupling mirror (OCM) reflectivity (R), the Cr^{4+} :YAG initial transmission (T_i), the Nd:YAG doping level and the resonator length, was performed. Finally, by combining a Cr^{4+} :YAG SA with $T_i = 0.40$ and an OCM of $R = 0.50$, the laser yielded pulses with energy over 6 mJ and pulse duration below 1.5 ns. The set-up was made of discrete elements, but it was pointed out that a monolithic design is necessary in order to finally design the laser spark in a robust form, able to withstand high thermal and mechanical stress. Such a laser-spark prototype can be seen in Fig. 2 [23]. Additional optimization work was performed by the same group from TUW, Austria, in order to control the laser pulse energy and the number of pulses that are generated within a pump pulse [38].

In parallel with the researches made at TUW in Austria, LI was also investigated with outstanding results at the Institute for Molecular Science (IMS), Okazaki, Japan, by the group led by T. Taira. Based on previous works done at IMS [39,40], one of the first micro-chip passively Q-switched lasers was built by Tsunekane et al. [41]. The laser was made of distinct elements, a 1.1-at.% Nd:YAG, a Cr^{4+} :YAG SA with $T_i = 0.30$ and an OCM of reflectivity $R = 0.50$. It had a short 10 mm length and was encapsulated in a temperature stabilized module. Laser pulses with 3 mJ energy and 1.2 ns duration at 10 Hz repetition rate were generated with a pump pulse of 120 W peak power and duration slightly above 100 μs . A 4-pulse train (12 mJ total energy) could be obtained by increasing the pump pulse duration to 500 μs . This newly-developed micro-laser was used to ignite $\text{C}_3\text{H}_8/\text{air}$ (propane/air, stoichiometric mixture) in a constant-volume combustion chamber. A faster development of the flame kernel was observed for LI in comparison with classical electric spark ignition, due to the absence of quenching effects induced by the conventional spark plug electrodes.

A passively Q-switched Nd:YAG- Cr^{4+} :YAG laser with 1.2 MW peak power was reported by Sakai et al., in 2008 [42]. Pulses at 100 Hz repetition rate with the energy of 0.69 mJ and 580 ps duration in Gaussian transverse mode ($M^2 = 1.04$) were obtained. In addition, a set-up in which Nd:YAG and Cr^{4+} :YAG SA were contacted optically was realized. This device yielded pulses with 0.67 mJ energy and 400 ps duration (1.7 MW peak power) and could be considered a step forward realization of a laser spark plug based on Nd:YAG/ Cr^{4+} :YAG composite structure in monolithic design.

It can be observed (and worthwhile to note) that the strategy adopted by the IMS group was to use pulses with short (ns-order or below) duration; the energy of several mJ per pulse was therefore sufficient for LI. Such an Nd:YAG- Cr^{4+} :YAG micro-laser was reported by Tsunekane et al., in 2010 [43]. The device yielded 2.7 mJ energy per pulse at 600 ps duration and beam quality of $M^2 = 1.2$. Moreover, trains of four pulses with the total energy of 11.7 mJ were realized. The laser was used to study combustion of $\text{C}_3\text{H}_8/\text{air}$ (stoichiometric mixture, AFR = 15.2) in a constant-volume chamber at room temperature and atmospheric pressure. Moreover, reliable ignition (100% probability) was obtained by laser in a lean mixture (AFR = 17.2), where ignition by electrical spark plug failed. Ignition tests were also performed on a GDI automobile engine (1AZ-FSE, Toyota Motor Corp) [44]. In experiments the Nd:YAG- Cr^{4+} :YAG micro-laser was fixed on a metal frame close to the engine and the laser beam was directed by mirrors and then focused through an Al_2O_3 window in one of the engine cylinders, at the same point as an electrical spark plug. A single laser pulse with 2.3 mJ energy ignited the engine successfully with stoichiometric mixture of gasoline and air. Contamination or damage of the window was not observed after several hours of operation. A laser spark prototype with one-beam output that was realized at IMS, Okazaki, Japan is shown in Fig. 3a.

The advance in manufacturing laser materials by ceramic methods and in optically bonding of such all-polycrystalline media has enabled the use of composite structures to build the first laser spark-like devices with multiple-beam output [45–47]. The adopted strategies implied the use of multi-lines from fiber-coupled diode lasers to pump composite, all-ceramic Nd:YAG/ Cr^{4+} :YAG in monolithic design. A two-beam output laser was presented in 2011 [45,47] employing Nd:YAG/ Cr^{4+} :YAG composite media (Fig. 3b). In addition, while the initial transmission of Cr^{4+} :YAG SA was kept constant, at $T_i = 0.30$, Nd:YAG sides with various Nd-doping level were considered. Laser pulses with 2.5 mJ energy and 800 ps duration (corresponding to a peak power $P_p = 3.1$ MW) were measured from the 1.1-at.% Nd:YAG/ Cr^{4+} :YAG composite ceramic. A 1.5-at.% Nd:YAG/ Cr^{4+} :YAG yielded pulses with $P_p = 3.2$ MW (2.1 mJ energy, 650 ps duration) whereas the peak power was $P_p = 2.3$ MW (1.5 mJ energy, 650 ps duration) for a highly-doped 2.0-at.% Nd:YAG/ Cr^{4+} :YAG ceramic. All configurations were compact (with each composite Nd:YAG/ Cr^{4+} :YAG shorter than 11 mm) and air breakdown was obtained from each scheme. Further engineering has enabled the realization of a spark-plug like, composite, all-ceramic Nd:YAG/ Cr^{4+} :YAG monolithic laser with three-beam output, as shown in Fig. 3c [46,47]. The composite medium consisted of a 7.5-mm thick 1.1-at.% Nd:YAG that was bonded to a 2.5 thick Cr^{4+} :YAG SA with $T_i = 0.30$. The monolithic design was obtained by coating the resonator

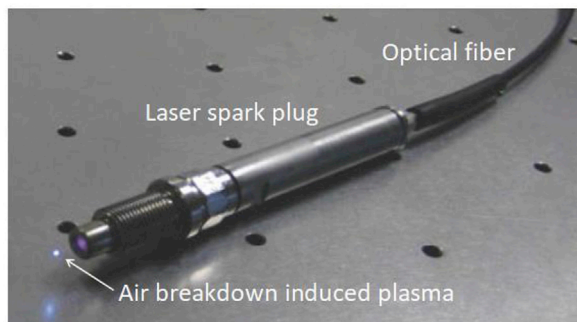


Fig. 2. A laser spark plug that was built based on a diode-pumped monolithic Nd:YAG/ Cr^{4+} :YAG laser design is shown [23].

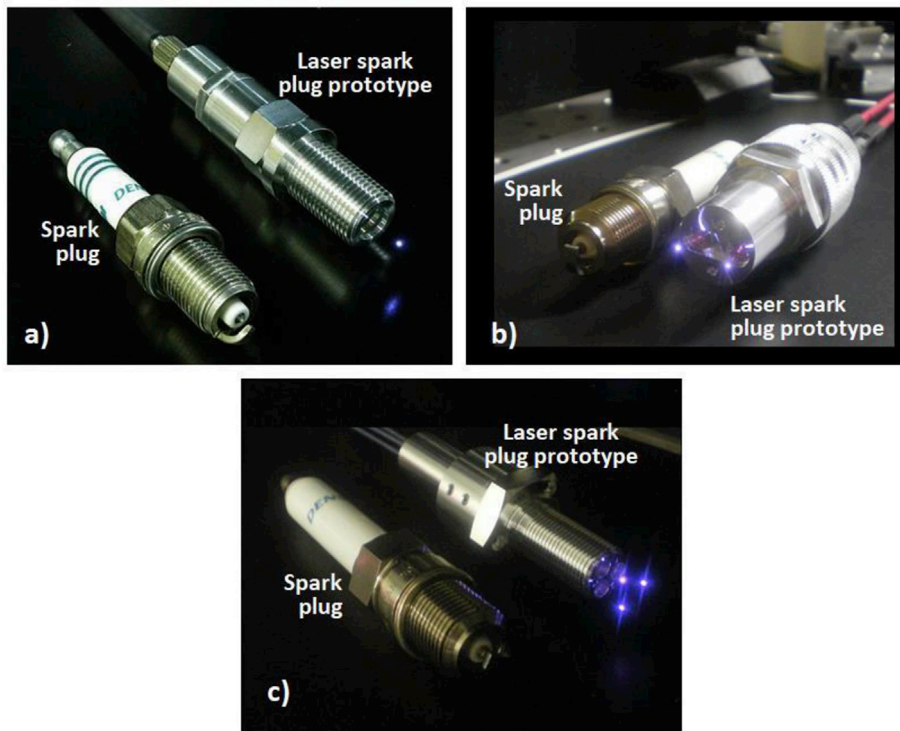


Fig. 3. Laser spark prototypes realized at IMS, Okazaki, Japan are shown: a) One beam, discrete elements (single-crystals Nd:YAG, Cr⁴⁺:YAG and resonator mirrors) [44,47], and composite all-ceramics Nd:YAG/Cr⁴⁺:YAG in monolithic design with: b) Two-beam output [45,47] and c) Three-beam output [46,47].

high-reflectivity mirror (HRM) on the free side of Nd:YAG whereas the OCM (with transmission $T = 0.50$) was deposited on the exit surface of Cr⁴⁺:YAG. For 5 Hz repetition rate the laser outputted pulses with the energy of 2.37 mJ and 2.8 MW peak power, in a beam with $M^2 = 3.1$. The pump pulse energy was 26.7 mJ. Very important, the ceramic medium, of 9 mm diameter, showed a very good uniformity; the standard deviation of the energy measured along Ox and Oy axes (at a 0.5-mm step) was below 3%. When the pump repetition rate was increased up to 100 Hz an increase by 6% of the laser pulse energy was obtained; the corresponding increase of the pump pulse energy, necessary to sustain laser emission, was also 6%.

Several other works done in the same research group are worthy of mention. An Yb:YAG medium was investigated as a solution for replacing Nd:YAG in a passively Q-switched laser with Cr⁴⁺:YAG SA [48,49]. A plane-convex laser resonator was used in order to enhance the fundamental mode size in the Yb:YAG rod (5-at.% Yb, 4.2 mm length). The system was pumped at 940 nm by a fiber-coupled diode laser that was operated up to 100 Hz in quasi-cw mode. Laser pulses with the energy of 3.6 mJ and 1.3 ns duration were obtained with a Cr⁴⁺:YAG SA of $T_i = 0.89$; the pulse peak power reached $P_p = 2.8$ MW. Although Yb:YAG presents some advantages (such as wide absorption band and low quantum defect between the pump and the laser wavelength), it requires a high-pump level for threshold operation. Moreover, the quasi-four level nature of Yb:YAG makes its output sensitive to temperature. Hence, it was concluded that Yb:YAG-Cr⁴⁺:YAG is not suitable for operation at temperatures >50 °C.

To further simplify the laser spark set-up, several configurations were evaluated, all involving end-pumping schemes. Thus, a fiber-coupled VCSEL was employed to pump a Nd:YAG rod through focusing lenses or directly from the fiber; the comparison was made with a thin-rod Nd:YAG that was pumped directly from the same fiber [50]. It was observed that the thin-rod Nd:YAG performs similarly with the Nd:YAG pumped through lenses. Laser pulses with energy larger than 1.5 mJ and 900 ps duration were obtained from a 1.0-at.% Nd:YAG thin rod (1.2 mm diameter, 4 mm length) and a Cr⁴⁺:YAG of $T_i = 0.40$, in a resonator with OCM of reflectivity $R = 0.50$. Very important, air breakdown was obtained and the VCSEL device could be operated on a large (20 °C–65 °C) temperature range without altering the laser pulse characteristics.

Results on the long-time operation of a composite all-ceramic Nd:YAG/Cr⁴⁺:YAG monolithic laser were reported by Tsunekane and Taira [51]. Laser pulse operation at 20 Hz repetition rate with 3 mJ energy and 1 ns duration was carried out at room temperature for 8000 h, without noticeable degradation. Only $\pm 3\%$ fluctuation in pulse energy was registered during the first 2000 h of operation, this being attributed to changes in ambient conditions. The experiment was also run at 80 Hz repetition rate for 7000 h. During these two tests, the temperature of the laser was controlled at 23 °C, while a trial at 20 Hz repetition rate and 90 °C laser temperature was also performed for 7000 h. Although investigations were not performed at higher temperatures or in conditions of vibration, the data nevertheless indicated good reliability for long-time operation of such a Nd:YAG/Cr⁴⁺:YAG micro-laser.

As an accomplishment of these researches, the LI of an automobile gasoline engine was reported in 2013 by Taira et al. [52]. The

laser spark plug developed and built for this had a passively Q-switched, monolithic, composite Nd:YAG/Cr⁴⁺:YAG all-polycrystalline medium. It had a rectangular shape and consisted of 1.0-at.% Nd:YAG that was bonded to a Cr⁴⁺:YAG with $T_i = 0.30$; the medium length was 10 mm. When pumped with pulses of 500 μ s duration, the laser yielded single pulses with 2.4 mJ energy; whereas, by increasing the pump pulse energy, trains of four-pulses with total an energy of 9.6 mJ could be obtained. The duration of a single-laser pulse was 700 ps. The ignition tests were performed on a real 1.8-liter gasoline, straight four-piston automobile engine with GDI. The diode lasers and the cooling systems were placed in the automobile trunk; stainless-steel pipes were employed to protect the optical fibers between the diode lasers and the laser spark plugs. In addition, the laser spark plug temperature was kept at 20 °C using a water cooling system. Under these conditions, the automobile was successfully powered by LI alone. Further measurements, performed at 1200 rpm speed and 73 N·m load, showed improved operation under LI in lean air-fuel mixtures with an equivalent ratio AFR in excess of 22. Importantly, the laser pulse energy (of 9.6 mJ) was lower than that of a conventional spark plug (35 mJ).

The works mentioned previously made use of end-pumping schemes to realize laser devices suitable for LI. An alternative solution was adopted by Kroupa et al. in 2009 [53]: A side-pumping geometry was employed to demonstrate a compact and robust passively Q-switched Nd:YAG-Cr⁴⁺:YAG laser with high 25 mJ energy per pulse at repetition rates up to 150 Hz. The laser was built with a 1.1-at.% Nd:YAG rod of 32 mm length that was side-pumped with array diode lasers, Cr⁴⁺:YAG SA with $T_i = 0.15$ for Q-switch and an OCM, all distinct elements. The configuration length was 170 mm, quite considerable, but it allowed delivering of laser pulses with duration of 3 ns. Thus, this approach decreases the probability to damage coatings or the optical elements. All optical components were sealed together with a focusing lens in a housing that withstands mechanical and thermal shocks of an internal combustion engine (Fig. 4a). Furthermore, the pulse-to-pulse variation of the laser pulse energy was less than 5%. A decrease of the laser pulse energy was observed, however after several million shots. This was attributed to the damage threshold of the coatings, designed for 1.5 GW/cm². As a solution, coatings with threshold higher than 3 GW/cm² were investigated. Engine tests were performed with a single glass-cylinder AVL motor fixed on a stand. Important, the laser head was mounted directly on the engine (in a protective steel tube). The engine was operated in homogeneous as well as in stratified mode, in order to test the ignition process properties in both regimes. Iso-octane and heptane were used as fuels, with the air-to-fuel ratio being varied from stoichiometric $\lambda = 1.0$ to $\lambda = 1.5$. The ability of the laser to ignite lean mixtures was proved: Thus, while misfiring was observed with an electrical spark plug at $\lambda = 1.3$, the laser was able to induce ignition until $\lambda = 1.5$.

Work was carried out at Carinthian Tech Research, Villach in Austria to improve such a side-pumped Nd:YAG/Cr⁴⁺:YAG laser (referred to as HiPoLas[®]). Miniaturization of the laser was achieved using a monolithic resonator and integration of all optical components within the laser head [54]. The diode lasers were mounted around the cylindrical Nd:YAG rod in a hexagonal geometry and stabilization of the diode wavelength achieved using volume Bragg gratings. The laser medium was a composite Nd:YAG/Cr⁴⁺:YAG structure (single-crystal nature for both components), with the HRM mirror coated on the free side of the Nd:YAG rod and the OCM deposited on the free surface of Cr⁴⁺:YAG. In a first design, cooling of diode lasers and Nd:YAG/Cr⁴⁺:YAG was by re-circulating liquid, an approach that allowed operation up to 100 Hz repetition rate (Fig. 4b). In this scheme, the laser yielded pulses with 55 mJ energy and 1.8 ns duration, with an overall optical-to-optical efficiency of 0.19. Lifetime tests were performed at 45 mJ pulse energy, showing no

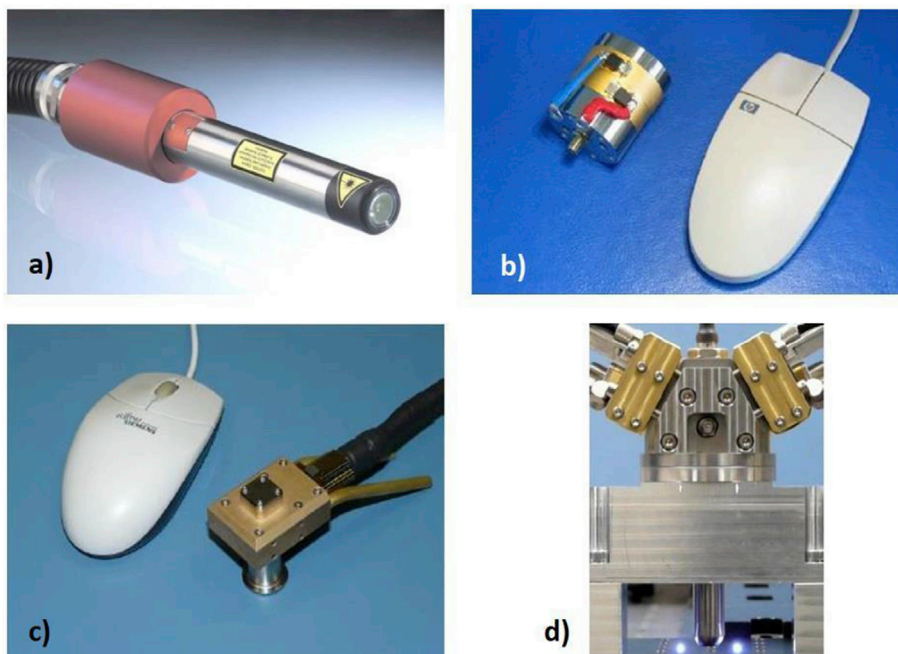


Fig. 4. The HiPoLas Nd:YAG laser system. a) The first laser igniter with housing and focusing lens [53]. Laser design with: b) Ring-type water cooled chamber [54,55] and c) Ultra-compact chamber with passive or active cooling [54]. d) A laser head is generating plasma at two locations [56].

degradation of the coatings for up to several million pulses. A second design considered further optimization of the laser for minimum size, using integrated thermal electric elements for passive or active cooling (Fig. 4c). In this case, laser pulses with the energy of 35 mJ and 2.0 ns duration were obtained. The laser spark plug also contained a lens for beam collimation (positioned directly after the OCM) and a plane-spherical sapphire lens for beam focusing. The plane side of the focusing lens acted as a window to the combustion chamber. The lenses were soldered in tubes made of ceramic or Kovar steel and the tests concluded that this arrangement could withstand chamber pressures of up to 250 bar at temperatures of up to 400 °C. The laser system was tested on different engines, namely: a) a stationary gas engine operated at speeds up to 3000 rpm, in which ignition was successful across a broad range of AFRs; b) an aerospace turbine with kerosene injection, though in this case with less success, and c) rocket engines using oxygen and hydrogen fuel. The laser was operated on rocket thrusters with high acceleration levels, up to several hundred G, without degradation. Recently, the use of the HiPoLas laser enabled the realization of an LI system that could generate plasma at two redundant locations (Fig. 4d). Further, an advanced laser concept based on the HiPoLas, in combination with an additional amplifier stage, yielded laser pulses with energy up to 70 mJ in laboratory tests and 55 mJ in an integrated prototype [55]. In conclusion, the HiPoLas[®] Nd:YAG laser has proved to be one of the most successful sources designed for LI, with (in principle) potential application to the ignition of gas engines and rocket engines [56].

A side-pumping scheme was also used by Ma et al. [57] to build a passively Q-switched Nd:YAG-Cr⁴⁺:YAG laser. Different to other developed lasers, this device was operated in pulse-burst mode to output 8 pulses per burst at 10 Hz repetition rate or 6 pulses per burst at 100 Hz repetition rate. The energy per pulse was 15.5 mJ and 13.9 mJ, respectively, and the single-pulse duration was 13.3 ns. The laser beam quality was characterized by $M^2 = 4.1$. An improved version of this first laser (that addressed thermal lensing in the Nd:YAG crystal) yielded 6 pulses per burst at 100 Hz repetition rate, with 1.6 mJ energy and 14.2 ns duration per each pulse. The beam quality factor was reduced to $M^2 = 2.2$. Such a laser device looks promising for LI, although improved compactness is considered as being necessary.

In attempting to present chronologically the achievements in the field of LI, the work of Robert Bosch GmbH should be mentioned at this point. The first investigations on LI were done at this company in the 1970's, followed up by increased research and development activities after the year 2000 [58]. LI systems were built and tested for ignition of automobile GDI engines and for stationary gas engines. Innovations were focused on function, quality and costs. Solid-state lasers with bonded YAG crystals of large diameter were produced and endurance tests of 10000 h were conducted. Technological methods for integration of the laser in a compact housing were found; tests were performed to seek solutions to the window fouling resulting from deposition of soot, oil ashes and particles; and the durability of Bosch LI systems on stationary gas engines was demonstrated. The investigated pump concepts were based on a) edge emitters (diode laser array) in combination with an optical fiber; and on b) a VCSEL in combination with simple pump lenses [59]. Laser pulses with energy between 2 mJ and 6 mJ were realized with the first pump choice. The use of the VCSEL allowed a simpler set-up and increased the laser pulse energy up to 10 mJ. A series of patents could be mentioned, for example [60]. In conclusion, Robert Bosch GmbH can offer several prototypes to engine manufacturers and may start further developments as soon as the market shows interest in this new technology (perhaps a not very optimistic statement).

A study of the influence of temperature on the laser pulse characteristics obtained from a Nd:YAG-Cr⁴⁺:YAG laser was done by Dascalu and Pavel [61]. A single-crystal Nd:YAG (0.7-at.% Nd) and a variety of Cr⁴⁺:YAG SA single crystals with initial transmission T_i between 0.30 and 0.60 were used in experiments. For each Nd:YAG-Cr⁴⁺:YAG combination the set-up temperature was varied between 25 °C and 150 °C with an oven. Improvement of the laser pulse energy with increasing temperature was observed, with no detectable influence on the laser pulse duration. Higher pump pulse energy was, therefore, necessary in order to sustain laser emission. Changes in T_i of a Cr⁴⁺:YAG SA were not observed. Thus, the variation of Nd:YAG emission cross section with temperature and changes in resonator configuration due to thermal effects were considered the main reasons for the change of laser pulse energy with temperature. More data obtained with a Nd:YAG-Cr⁴⁺:YAG laser that was operated at high temperatures with normal coated OCMs, as well as with a volume Bragg grating (VBG) optical element as an output coupler, were published by Pavel et al. [62]. These results were considered valuable for the design a laser spark plug that could be used, in principle, on an automobile engine.

The results of a study performed at INFLPR on the ignition induced in methane-air by the classical spark plug and by an electro-

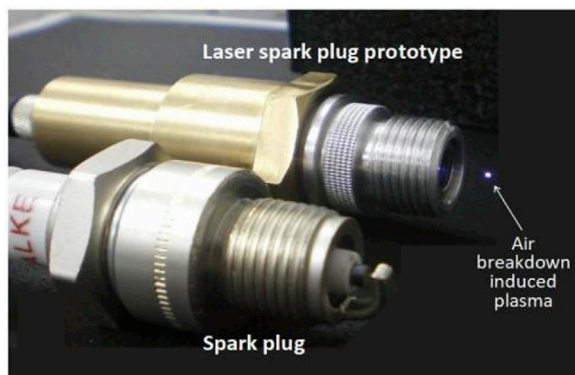


Fig. 5. A preliminary laser-spark prototype realized at INFLPR in 2011 is shown.

optically Q-switched Nd:YAG laser was reported by Salamu et al. [63]. Several parameters of the ignition, like peak pressure, pressure rising time and speed propagation of the flame front, were recorded in a constant volume chamber. A preliminary laser-spark prototype that was built with a composite Nd:YAG/Cr⁴⁺:YAG ceramic medium was also tested in these experiments. A view of this first prototype developed at INFLPR can be seen in Fig. 5.

A composite Nd:YAG/Cr⁴⁺:YAG medium that was end pumped with a fiber-coupled diode laser in quasi-cw mode is the main configuration chosen to realize a laser spark plug suitable for the use on an automobile engine. A new laser scheme for such a device was proposed by Dascalu et al., in 2013 [64]. In this design the Nd:YAG medium is square shaped and the pump is introduced directly into it from the fiber end through a 90° isosceles optical prism (Fig. 6a). The prism is positioned on one of Nd:YAG lateral sides, at one of the medium extremities. This laser scheme, named by “laterally pumped by a prism laser” has several advantages, like simplicity, less optical elements in comparison with an end-pumped laser, easy alignment, or improved compactness. Furthermore, the pump light is not absorbed in Cr⁴⁺:YAG SA (and thus do not influence the parameter T₁), so the SA medium can be positioned to either side of Nd:YAG, offering freedom for the laser resonator design. For operation in free-generation regime a 1.0-at.% Nd:YAG crystal (10 mm long, 1.5 × 1.5 mm² square shape) was considered (Fig. 6b). Laser emission with a slope efficiency of 0.51 was realized, very close of the performances (0.60 slope efficiency) obtained when the same medium was end pumped through a set of two coupling lenses [65]. The integration of such a geometry was done with a composite Nd:YAG/Cr⁴⁺:YAG ceramic medium, using a Cr⁴⁺:YAG SA with T₁ = 0.85. Q-switched laser pulses with 0.29 mJ energy and 11 ns duration have been measured [66]. Thus, this design (Fig. 6c) showed promising features. Further work has to be performed, however, in order to optimize the scheme and make it suitable to deliver pulses with higher energy and shorter duration, suitable for laser ignition.

Ignition of an automobile engine was reported by N. Pavel et al., in 2015 [67]. The laser spark device was an improved version of the first prototype developed at INFLPR by the same group. A figure of this new laser spark is shown in Fig. 7a. Following laborious design work, the device was built such to deliver pulses with the energy of 4.0 mJ and duration of 0.8 ns. The interface between a laser spark and the engine cylinder was a sapphire window of 2.0 mm thickness, able to withstand static pressures higher than 20 MPa. All optical components (including the window) were fixed in a metallic body with an epoxy adhesive that poses high shear and peels strength, and that could operate on a broad temperature range (−70 °C–170 °C). The LI experiments were performed on a Renault engine (K7M 812 K type, 1.6 litre gasoline) with multi-point injection system that was mounted on a test bench. The ignition triggering of the integrated four-laser spark system was done directly from the electronic control unit (ECU) of the engine. A photo of the Renault engine that was equipped with the LI system is presented in Fig. 7b. Various parameters of the engine operation were determined. The in-cylinder pressure was measured with an AVL GU-21D piezoelectric transducer mounted on one of the engine cylinders. Exhaust gases were sampled from the valve gate with a Horiba Mexa 7100 analyzer. Data acquisitions were made on 500 consecutive engine cycles, for engine speeds in the range 1500–2000 rpm and applied loads of 770 mbar, 880 mbar and 920 mbar (in this case, the load was the absolute pressure from the intake manifold). The engine was running near a stoichiometric AFR (λ~1).

Table 1 presents comparative results regarding the stability of the engine that was operated by classical spark plugs and by LI. BSFC is Brake Specific Fuel Consumption parameter and COV_{Pmax} represents the coefficient of variability of maximum pressure. It is worthwhile to comment that a fair comparison should be made for similar BSFC. As it can be seen from Table 1, LI improved COV_{IMEP} by 22.6% and COV_{Pmax} by 15.8% at 1500 rpm speed and moderate 880 mbar load. The influence of LI on engine stability was less at high speed and load; this behavior was expected as cyclic variability of an engine ignited by a classical spark plug in these conditions is also improved in comparison with operation at low speeds and loads. In the case of exhaust emissions, lower CO and HC were measured for the engine ignited by laser spark plugs.

Thus, as it was summarized in Table 2, the decrease of CO for LI was in the range of ~18%–~25% for all investigated regimes.

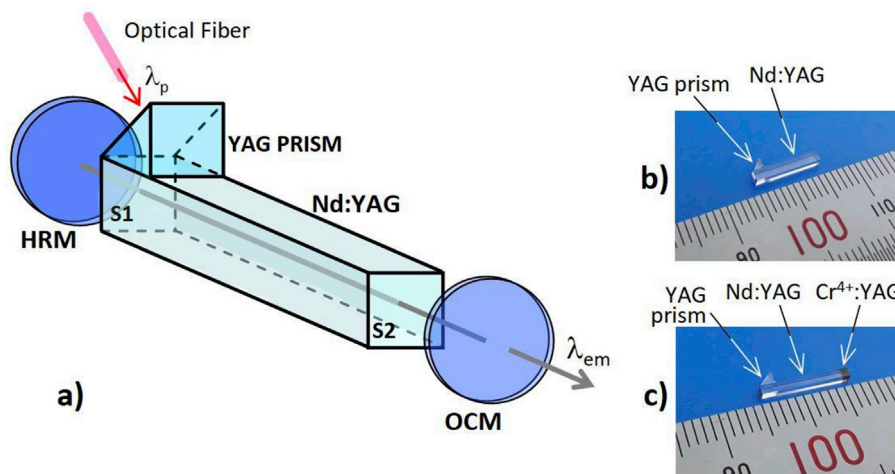


Fig. 6. The Nd:YAG laser pumped laterally through a YAG prism is shown [64–66]. a) The laser schematic for operation in the free-generation regime. Cr⁴⁺:YAG can be positioned either between HRM and side S1 of Nd:YAG or between side S2 of Nd:YAG and OCM. b) The YAG prism-Nd:YAG structure. c) The YAG prism-composite Nd:YAG/Cr⁴⁺:YAG configuration. λ_p : the pump wavelength; λ_{em} : the laser wavelength.

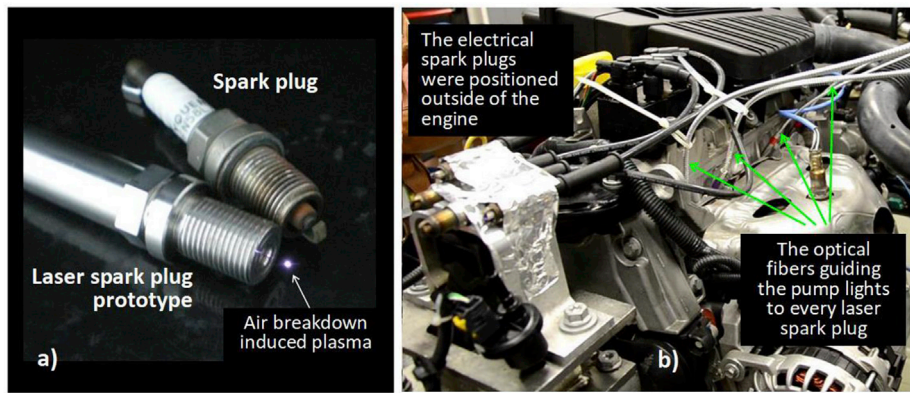


Fig. 7. a) A laser spark plug developed at INFLPR. b) A Renault engine ignited entirely by laser sparks.

Emissions of HC at 1500 rpm were lower by ~14%~17% for LI whereas this improvement was smaller (3%~4%) at higher 2000 rpm speed. These improvements were associated with more efficient combustion under LI, meaning better oxidation of the carbon and hydrogen atoms in the fuel. On the other hand, an increase of NO_x was measured, of ~8% at 1500 rpm speed and about 2% at 2000 rpm speed. This was explained by a higher flame temperature in the first part of combustion when much NO_x is produced. The increase of CO₂ under LI was expected, as the amount of carbon entering into and then evacuated from the combustion chamber is constant. Based on measurements it was concluded that the power of the LI engine increased by ~1.7% at 1500 rpm speed and by ~3% at 2000 rpm speed in comparison with the classical electric ignition.

One important issue for laser ignition of an engine is the combustion deposits that form on the inner side of the window that acts as an interface between the engine cylinder and the laser spark plug. Studies as early as 2003 [68] using ns pulse Nd:YAG lasers showed that, in principle, ‘self-cleaning’ of the inner window surface by the pulsed laser radiation is possible, by mechanisms of either ablation or shock cleaning. A more detailed study by Ranner et al. [69] showed that laser ablation can indeed be used for cleaning the window. Here, it was shown experimentally that a few laser shots (or even a single one) of optimum fluence can keep the window free of deposits. Furthermore, a high temperature of the window surface from the combustion chamber is preventing deposition of some organic products, e.g. soot [23]. During the LI of the automobile engine [67] the engine was triggered twice per cycle, by applying laser pulses in cylinder ‘4’ (on the exhaust stroke) while the ignition was realized in cylinder ‘1’. Thus, it was considered that the window of cylinder ‘4’ was cleaned (at least partially) before a new ignition. The same procedure was applied for cylinders ‘2’ and ‘3’. A similar method using ‘redundant spark’ laser pulses was described by Mullet et al. [22]. In addition, in Ref. [67] the pump pulse length was increased (from time to time) such to obtain two laser pulses from a laser spark plug. It was considered that in this way the first laser pulse can help to clean the window whereas the second laser pulse initiates the ignition. Using these methods (although not clear which was more important) the engine car was running without problems during the experiments (of few hours duration).

Further data on fuel consumption and stability of a similar Renault engine that was ignited by laser spark plugs at different air-fuel mixtures were presented by Birtas et al [70,71]. Measurements were performed at 2000 rpm speed and break-mean effective pressure (BMEP) between 2.0 bar and 8.0 bar. Importantly, optimum advance curves for LI were determined for each investigated point. For operation at 2 bar BMEP and λ = 1.02 (i.e. near stoichiometric air-fuel mixture) the fuel consumption decreased by ~3.4% for LI in

Table 1

Engine stability for LI. Sign (–) and (+) indicates a decrease (an improvement), respectively an increase of the given parameter, in comparison with standard ignition by electrical spark plugs [67].

Speed (rpm)	Load (mbar)	BSFC (%)	COV _{IMEP} (%)	COV _{Pmax} (%)
1500	880	0	–22.6	–15.8
	920	–0.4	–18.5	–15.1
2000	770	0.8	–14.6	–10.2
	920	0.4	+2.5	–2.6

Table 2

Emissions for ignition by laser spark plug and standard ignition by electrical spark plugs [67].

Speed (rpm)	Load (mbar)	BSFC (%)	CO (%)	HC (%)	NO _x (%)	CO ₂ (%)
1500	880	0	–22.4	–14.4	+8.0	+0.7
	920	–0.4	–21.9	–17.5	+7.6	+0.8
2000	770	0.8	–18.7	–3.8	+1.6	+1.1
	920	0.4	–25.1	–3.0	+2.6	+1.1

comparison to electric spark ignition (Fig. 8a). This difference was less pronounced for lean mixtures ($\lambda \sim 1.21$). On the other hand, the coefficient COV_{IMEP} had similar values for both LI and classical ignition near stoichiometric mixture ($\lambda \sim 1$), but was improved at leaner mixtures. For $\lambda \sim 1.21$ the coefficient COV_{IMEP} was better by $\sim 32\%$ for LI. A comparison of consumption at $\lambda \sim 1$ and different loads was made at 2000 rpm speed. As shown in Fig. 8b, the improvement in fuel consumption reduced when BMEP was increased and eventually no difference was detected for BMEP more than 7.0 bar [72]. Differences between the duration of combustion for these two types of ignition were also evaluated with the engine running steady near stoichiometric ($\lambda \sim 1$) air-fuel ratio [70]. Shorter durations for combustion were determined for LI, mainly at medium engine loads (BMEP values between 4 bar and 5 bar). For example, the combustion duration with LI at 5 bar BMEP was at least 30% shorter than the burning duration using standard ignition. These shorter combustion durations when using LI leads to a decrease in the level of detonation; the use of a higher spark advance for LI can, therefore, increase the engine efficiency in comparison with the classical ignition.

Following all these investigations and results, a Renault car was ignited and moved only by laser spark plugs [72]. The automobile was a Dacia vehicle that was equipped with a K7M 812 k engine, a naturally aspirated indirect injection gasoline engine with four cylinders in line, capacity of 1598 cm³, nominal power of 62 kW, maximum torque of 135 N m and 9.5 compression ratio. The engine that was equipped only with laser spark plugs is shown in Fig. 9a whereas the car returning after a travel trip can be seen in Fig. 9b. The classical spark plugs that were positioned near the engine (under the hood) are visible in Fig. 9a. The authors considered this subject still an attractive research area, although the price of an LI system, not yet competitive, could influence further advancements in this field and implementation of such ignition solution in the real automobile world.

3.3. The pump with VCSEL of a laser ignition system

Most laser systems presented previously were pumped in end or side schemes with diode lasers (fiber coupled or diode array lasers). In general, a diode laser is sensitive to temperature, showing a few nm wide emission spectrum that varies with temperature, usually of the order ~ 0.3 nm/K dependence. Considering the narrow absorption band of Nd:YAG around 0.81 μm (less than 3 nm width), a change in ambient temperature of several degrees (even up to 10 °C) can shift the diode emission wavelength out of the Nd:YAG absorption spectrum. Therefore, stabilization in temperature of the diode laser emission wavelength is necessary. This can be realized by several methods, such as internal distributed feedback (DFB) or the use of an external VBG. Alternatively, the diode laser used for pumping can be replaced with another source, for example a VCSEL laser. A large number of reports can be found in the literature on the design, realization, improving and optimization of VCSELs as well as various applications of the devices. For example, an 804 nm emitting VCSEL was used to excite, in an end-pumping geometry, a passively Q-switched Nd:YAG-Cr⁴⁺:YAG laser [73]. Importantly, the coupling of the pump beam into the Nd:YAG rod was made with better than 98% efficiency using a single lens. Laser pulses at 5 Hz repetition rate with adjustable energy between 9 mJ and 18 mJ were obtained at 1064 nm, with the respective pulse durations being 3.7 ns and 4.6 ns. VCSELs offer uniform beam profile, narrow spectral line-width and 2D power scalability, making the device an excellent pump source for solid-state lasers. Results on the scalability of passively Q-switched Nd:YAG-Cr⁴⁺:YAG lasers pumped by a VCSEL array with emission at 808 nm were reported by Xiong et al. [74]. Q-switched performance obtained by end pumping in single- or dual-scheme, as well as side-pumping, were evaluated.

The low temperature dependence (~ 0.06 nm/°C) of its emission wavelength makes the VCSEL a very interesting source for building future LI systems. The results of one of the first studies on the influence of ambient temperature on the performance of a passively Q-switched Nd:YAG-Cr⁴⁺:YAG laser were reported by Wintner in 2013 [75]. Tsunekane and Taira showed that a VCSEL is an attractive pump source for LI devices [76]. In their study, more than 60% of the radiation emitted by the VCSEL was absorbed in a Nd:YAG medium, although the ambient temperature varied over a wide range, 10 °C–70 °C. A prototype fiber-coupled VCSEL pump module was

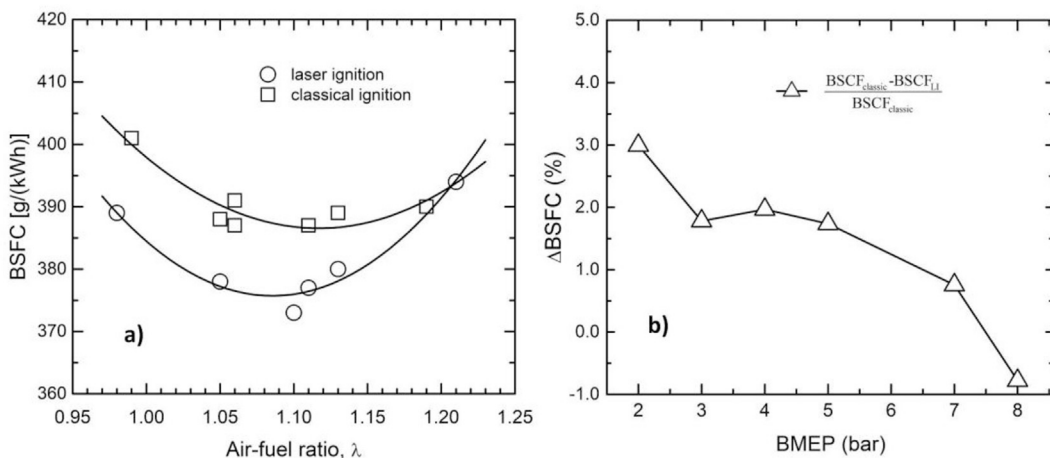


Fig. 8. a) BSFC versus air-fuel ratio λ , engine operation at 2000 rpm speed and load BMEP = 2 bar [70]. b) BSFC versus load BMEP, 2.000 rpm speed and air-fuel ratio $\lambda \sim 1$ [72].

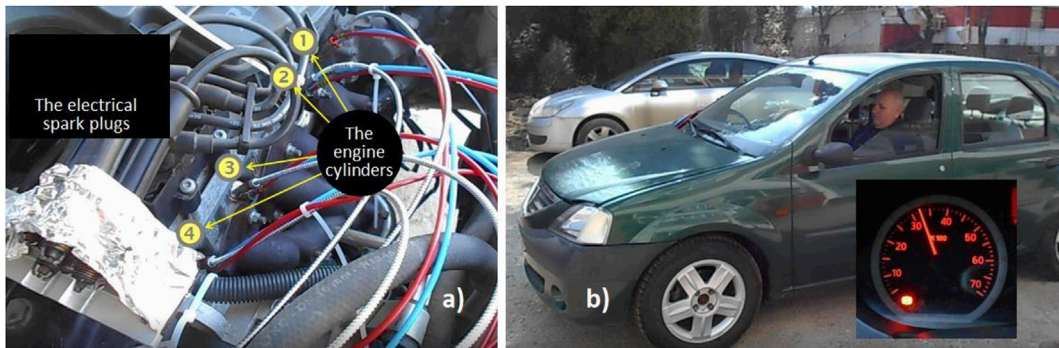


Fig. 9. a) The LI system mounted on the Renault engine is shown; the electrical spark plugs can be seen separately, left side of the figure. b) The Renault engine ignited by laser spark plugs is returning from a trip. Inset is a shot of the car speed meter [72].

also realized [76], consisting of a VCSEL light source (120 W quasi-cw operation), a micro-lens array and a focusing lens. Delivery of the pump laser beam through an optical fiber (0.91 mm diameter and $NA = 0.22$) was confirmed, with an optical coupling efficiency of 70%. As already mentioned, VCSELs were used by Robert Bosch GmbH as pumping sources for laser igniters [59] and by Tsunekane and Taira [50] to evaluate the performances of a Nd:YAG thin rod. According to the report of Gronenborn et al. [77], the optimization of the epitaxial design and of the geometrical array layout allowed a reduction of the required device dimensions by 50%. Pulses with 500 W peak powers were obtained from a VCSEL module with a diameter of only 23 mm; this size is small enough to be fitted in a laser spark plug that can be mounted directly on the engine. Thus, an integrated VCSEL pump module is seen as a potential alternative solution for delivery by the optical fiber of the pump beam from a remote diode laser to the laser igniter.

Significant research has been carried out (and is still underway) at RICOH Co., Japan towards realizing VCSEL pumped, passively Q-switched Nd:YAG/Cr⁴⁺:YAG lasers for LI, with high reliability and low cost. Such a Nd:YAG/Cr⁴⁺:YAG micro-laser that emitted pulses with 2.5 mJ per pulse and a burst of 4 pulses with the total energy of 10 mJ at 20 Hz repetition rate was reported in 2016 [78,79]. The laser pulse width was 460 ps (the pulse peak power reached 5.4 MW) and the beam quality was characterized by a factor $M^2 = 1.45$. It is important to mention that the pump solution involved the coupling of the VCSEL output to an optical fiber and then refocusing of the transmitted beam into the Nd:YAG medium [80]. In-house development of VCSEL and optical technology allowed realization of a fiber-coupled VCSEL module with high 200 W quasi-cw output power, the highest reported power at that time for such a system. Recent results presented by Ikeo et al. [81] showed even an increase of the laser device optical-to-optical efficiency, up to 19% from ~10% for the previously reported data [78–80]. Thus, for a similar pump pulse of 500 μ s width the optimized laser scheme yielded a train of 7 pulses with 2.71 mJ energy per pulse (19 mJ total energy per burst), each single laser pulse having 572 ps duration.

It is interesting to note that Princeton Optronics, USA now produces a high-power laser igniter (Fig. 10) that is pumped by a VCSEL [82]. Typically, the device emits laser pulses at 1064 nm with 12 mJ energy and 4.5 ns duration at 15 Hz repetition rate. The maximum parameters are 20 mJ energy per laser pulse and 5 ns duration at up to 20 Hz repetition rate. All these features are available for reasonably high temperature (50 °C) operation. Furthermore, the device has a compact and rugged design, and claims to be resistant to high levels of shock and vibration.

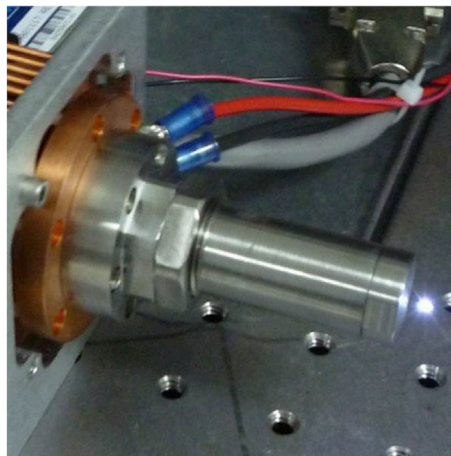


Fig. 10. High power VCSEL laser igniter of Princeton Optronics [82] (Courtesy Princeton Optronics).

3.4. Multi-point laser ignition

As has been mentioned, a main feature of LI is the ability to focus the laser beam at any position in the combustion chamber. Also, one important advantage is given by the possibility to induce simultaneous ignition in more than one location of the engine. Called multi-point ignition, this technique can shorten the distance that a flame has to cover during the combustion process. Consequently, the combustion time reduces and the flame will lose less heat than in the case of single-point ignition; hence, higher temperatures and pressures are reached, leading to improved thermal efficiency and increased power of the engine. Advantages of multi-point ignition are also seen in increased probability to fire lean air-fuel mixtures, in less heat losses for engines that use turbulence while running, or in the ignition of gas engines with large bore (just to list few of these advantages).

Influence of two-point LI combustion pressure and time of H₂-air and CH₄-air mixtures was studied by Phuoc [83]. Q-switched Nd:YAG lasers that operated at 1064 nm as well as at 532 nm, with a pulse duration of 5.5 ns, were used to ignite a constant volume chamber filled at an initial pressure of 760 torr. Single point and dual point LI were investigated, at different locations in the combustion chamber. The beam energy used for two-point LI was exactly half (9.25 mJ) of the 18.5 mJ laser pulse energy used for single point ignition. It was concluded that two-point LI increased combustion pressure and shortened the time of combustion in comparison with single point ignition, a benefit that could potentially be exploited for ignition of lean-fuel mixtures or in high-speed combustion applications.

A different approach for inducing LI is the conical cavity, a technique used first in 1999 by Morsy et al. [84] to study ignition in CH₄-air mixtures. In this novel approach, LI was obtained by launching the laser beam into a small conical cavity via multiple reflections from the cavity walls, thus without focusing the laser beam. A modified arrangement enabled LI in two-points [85]: The first ignition point (named 'spark ignition') was obtained by focusing the beam in the combustion chamber, while the transmitted laser beam was directed to a conical cavity to induce the so-called 'cavity ignition'. In experiments, a Q-switched Nd:YAG laser delivering pulses at 532 nm with tens of mJ energy and 7 ns duration was used to ignite CH₄-air mixtures at various initial pressures. It was observed that the ignition by classical spark plug and LI in one point has similar flame initiation time (defined as the time from laser shot to 5% mass burned). However, for LI in two points, the flame initiation period was reduced by 45%–69%, the decrease being more pronounced as the pressure decreased in the combustion chamber. Reduction of combustion time for two-point LI was observed, as the distance for the flame to travel is shorter (in comparison with ignition in one point). Morsy and Chung [86] have also reported LI of the hydrogen-air mixture in two points and three points by installing two conical cavities on a constant-volume combustion chamber. A Q-switched, frequency-doubled Nd:YAG laser (532 nm wavelength), with 360 mJ available energy and 7 ns duration pulses was employed. It was concluded that the pressure rise is much faster for the laser-induced two point cavity ignition, in comparison with both one-point laser-induced spark ignition and one-point cavity induced ignition. The time to reach maximum pressure was reduced slightly further for LI at three points. Reducing flame initiation period was considered to be an effective method to minimize cycle-to-cycle variation in an internal combustion engine, with direct application in lean-fuel burning systems. In addition, the fuel efficiency was expected to be improved by the use of a high compression ratio. A review of laser-induced multi-point ignition with conical cavities was presented recently by Chung [87]. Even five-point ignition was realized by adopting a conical cavity with an open end and a pre-chamber with additional holes. A reduction of total combustion time was determined for all investigated multi-point ignition schemes in comparison with ignition in one point by 'cavity ignition'.

Properties of hydrogen-air mixtures that were ignited by a laser beam in two points and three points were reported by Weinrotter et al. [13]. Hydrogen-air mixture with air-fuel equivalence ratio $\lambda = 4$ (no knocking effects) at initial temperature $T = 473$ K and 1 MPa initial pressure was used. Significant faster combustion was observed for LI in two points in comparison with ignition in one point; the energy of each beam used in these experiments was 8 mJ with 5 ns duration. The time until the pressure reached maximum was shorter by 50% and the peak pressure was 7% higher for LI in two points. There was no difference observed between ignition in three points and one-point ignition. However, as a diffractive lens was used for focusing the laser beam in three points, it was considered that the three plasmas were realized to close to one other, so they were acting like one-point induced plasma.

Some other fundamental studies can also be mentioned. Thus, ignition of lean methane-air mixtures in two points placed close to each other was studied by Horie et al. [88]. Two-point LI of a single-cylinder naturally aspirated gas engine showed higher thermal efficiency and improved IMEP stability in comparison with LI in one point or with ignition by a classical two-point spark plug [89]. A four-stroke, single-cylinder Robin EH30-DS engine (Fuji Heavy Industries) was operated by Saito et al. [90,91] under nitrogen dilution condition and ignited by laser in two points. The engine output was increased by the two-point ignition, even in high-dilution conditions. The potential of a two- and three-point LI system to improve the lean operation limit was discussed by Grzeszik [92]. Decreased fuel consumption and lower NO_x emissions were the main findings for multi-point ignition of a one-cylinder engine that was operated at 1200 rpm speed and IMEP = 2.6 bar.

Several compact lasers yielding multiple beam output were realized. As it was already mentioned, the pump with independent lines was a solution to build monolithic, composite Nd:YAG/Cr⁴⁺:YAG all-poly-crystalline lasers with two and three beams [45–47]. More recently, Ma et al. [93] have developed a passively Q-switched Nd:YAG-Cr⁴⁺:YAG laser with four-beam output. The technical solution was to pump through a 2 × 2 micro-lens array a 1.0-at.% Nd:YAG ceramic medium (6 mm thickness, 10 mm × 10 mm square shape); Cr⁴⁺:YAG SA with initial transmission $T_i = 0.80$ was employed. The laser also operated in burst mode, yielding two up to five pulses in each beam. The energy of a single-pulse laser in pulse burst was in the range of 0.12 mJ–0.22 mJ (quite low) whereas the duration was long, from 10.5 ns to 11.5 ns. A quasi-cw, diode-pumped, passively Q-switched monolithic, composite Nd:YAG/Cr⁴⁺:YAG laser with four-beam output was realized by Dascaiu et al. [94]. An optical system consisting of a focusing lens and a folding 90° isosceles prism was used for each independent pump line in order to keep the design compact. Each laser beam had greater than 3 mJ energy per pulse and pulse duration shorter than 0.9 ns; emission with a repetition rate between few and up to 60 Hz was investigated. Several lenses

were combined in the focusing line, such to focus the beams in the same plane or at different distances from the laser and with variable distances between the ignition points. Besides automobile engine ignition, it was argued that such a laser could be of interest for space propulsion systems or for ignition in turbulent conditions specific to aeronautical combustion.

Although promising, none of the laser devices with multiple-beam output mentioned above have been used (to the author's best knowledge) for ignition of a real engine. Most probably the compactness must be improved and the system resilience to various factors (like temperature and vibrations) is still weak. Nevertheless, another method that was investigated at the University of Liverpool used diffractive optics to generate multiple-beam output proved more successful. There, several sparks with an arbitrary spatial location in three dimensions were created by variable diffraction of a pulsed, single-beam laser [95] achieved with a spatial light modulator (SLM). A lamp-pumped, Q-switched Nd:YAG laser with emission at 1064 nm, ns duration pulse and adjustable energy per pulse was used in the experiments. The SLM (Holoeye LC-R 2500), on which computer generated holograms (CGHs) were displayed, was used to produce multi-beam patterns by diffraction, with an algorithm based on gratings and lenses applied to modulate the phase of the incident laser beam. The multi-beam pattern was then directed toward an optical plug and focused by a sapphire plane-convex lens to generate multiple focal points, dependent on the available Nd:YAG laser pulse energy. For example, three air breakdown sparks could be obtained with a laser pulse of nearly 60 mJ energy. With the CGH refresh rate being faster than the engine cycle time, this solution enables dynamic control of the geometric layout of multi-beam patterns during each combustion cycle. Such a multi-point ignition set-up is shown in Fig. 11a.

For the first time this method of generating multi-point laser sparks was applied to a single-cylinder automobile research engine (776 cm³ swept volume, 100 bar high pressure fuel delivery) [96]. Three-point laser sparks were obtained with either axial (Fig. 11b) or lateral (Fig. 11c) spacing. More stable combustion was obtained with multi-point LI when the engine was operated with lean air-fuel mixture (λ as high as 1.5). Extensive investigation on the performances and limits of such a method to generate multi-point laser sparks and further results of LI tests that were performed on the same single-cylinder automobile engine were reported recently by Kuang et al. [97]. Several questions to be answered were considered, like: a) how to deliver the multi-beam diffracted pattern into the engine cylinder through a hole that fits a classical spark plug; b) which is the maximum energy that an SLM can handle and how many sparks can be created; c) would the multi-location spark be of enough intensity and stability to ignite the engine, or d) how would the multi-spark ignition influence the engine performances in comparison with LI in one point. Optical damage experiments concluded that maximum safe energy to avoid damaging of SLM was 60 mJ (at 532 nm wavelength). It was then found that such energy is not sufficient to guarantee reliable (100% probability) ignition in three points; the tests on the real engine were therefore performed with two-point sparks that were laterally spaced by 4 mm. In the experiments the engine was run at 1000 rpm speed with lean air-fuel ratio; data were recorded for 500 consecutive cycles. Dual-point LI assured less misfiring than LI in one point for $\lambda > 1.05$. Ignition by classical spark plug could not run properly for $\lambda > 1.2$, but the engine was operated up to $\lambda = 1.45$, even with LI in one point. Furthermore, dual-point LI allowed engine operation (at lean air-fuel mixtures) with higher engine power and better engine stability in comparison with one-point LI. The results of this study are considered essential and could trigger future investigations for development and exploitation of compact laser systems suitable for engine ignition.

3.5. Additional facts. Laser ignition of natural gas reciprocating engines

The body of research in the field of LI has been significant and here some other approaches, methods and results should be mentioned. For example, Kojima et al. [98,99] attempted to control the process of plasma formation and the plasma flow by fs-laser pulses (provided by a Ti:sapphire laser) that were concentrated near the position where the beam of a Nd:YAG laser (with ns laser pulses) was focused. The influence of Ti:sapphire laser beam on the breakdown threshold energy induced by the Nd:YAG laser or on the position

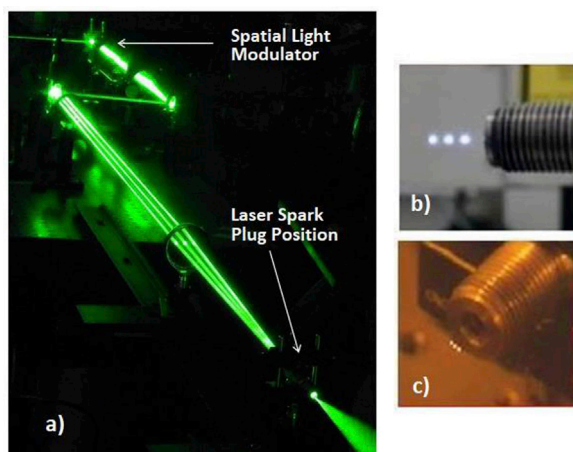


Fig. 11. a) A multi-point ignition offline test is shown. The three-point plasma generated in air by spatial light modulator with both b) axial and c) lateral spacing [96].

where plasma is initiated and how the plasma distribution changes was investigated; the impact of these findings on the LI ability to burn lean air-fuel mixtures were highlighted. The ignition of spray (specific to aeronautical operation conditions) was studied by Beheran et al. [100] with a double-pulse method. In these experiments the beams of a two Nd:YAG lasers (frequency-doubled at 532 nm wavelength) were focused through the same optical system with a variable delay (hundreds of ns to hundreds of μ s) whereas the energy ratio between the two beams was varied to maintain constant total energy. The influence of the laser beams on spark formation was determined. An extensive study on the LI with pulse trains on the flame formation in engine-like conditions was performed by Lorenz et al. [101]. The experiments were done in an optically accessible combustion chamber that was filled with CH₄/air mixture up to 1.0 MPa pressure. LI was realized with prototypes of laser spark plugs provided by Robert Bosch GmbH. Influence of fluid flow on the ignition process was investigated by igniting the fuel mixture above a jet nozzle. The analysis was focused on the interaction of consecutive pulses on the ignition process, including energy transfer characterization, analysis of laser-induced plasma, as well as description and analysis of shock-wave propagation and flame-kernel formation. Details will be given in the continuation of this review work (section 4). In recent work, Hsu et al. [102] used a high-repetition rate ns-laser to reduce the MIEs needed for LI from individual laser pulses by ~ 10 times, while maintaining comparable total energy. A significant increase in the ignition probability of lean combustible mixtures (air-isobutane and air-ethylene) in high-speed flows was also reported.

A study carried out by Mullett et al. [103] considered the influence of several laser beam parameters (energy, transverse mode, beam-waist size, the volume of the laser beam in the focal region) on the performance of an internal combustion engine. One-cylinder of a 1.6 liter test engine was ignited by a Q-switched Nd:YAG laser beam (1064 nm wavelength, 10 ns pulse duration), with the other three engine cylinders being ignited by electric spark plugs. It was found that LI performed better than classical ignition in terms of combustion stability (COV_{IMEP} and Var_{PPP} parameters). LI of compressed natural gas-air mixtures was investigated in a constant-volume combustion chamber as well as in a single-cylinder engine by Srivastava et al. [104,105]. The effect of the focal size of the focused laser beam and of the laser pulse energy on the engine combustion, performance and emissions were studied using different air-fuel mixtures. Lorenz et al. [106] and Bärwinkel et al. [107] have investigated the energy transfer optical breakdown induced in the air with end-pumped, miniaturized, passively Q-switched laser spark plugs. The influence of focal point features on energy transfer from the laser to plasma and the plasma formation and propagation were considered. Details of this work are discussed later in section 4.

Pioneering work done by McIntyre et al. [108–110] succeeded in the realization of an end-pumped, passively Q-switched laser igniter for lean-burn stationary natural gas engines. A fiber-coupled diode laser was used to pump axially (i.e. longitudinally) a Nd:YAG crystal that was Q-switched by a Cr⁴⁺:YAG SA. Laser pulses with 8 mJ energy and 2.5 ns duration (at 3.2 MW peak power) were obtained. The laser beam quality factor was $M^2 = 5.5$. The advantages of this scheme in comparison with a side-pumped passively Q-switched Nd:YAG-Cr⁴⁺:YAG system were highlighted. In order to transfer the laser beam into the engine, a sapphire window was brazed directly to the metal body of the spark plug as a first solution. A second approach was then the use of a fused silica lens (with a suitable thickness to handle high pressure), sealed with silicone rubber. Experiments were done on a Ricardo Proteus single-cylinder research engine [110], instrumented with several data acquisition systems. Emission measurements included O₂, total hydrocarbons, CO₂, CO and NO_x in the exhaust gas. Tests were performed with two fuels: natural gas, and a mixture of natural gas with hydrogen at several equivalence ratios. Furthermore, the engine speed was set at 1800 rpm and maximum brake torque timing was considered at each equivalent ratio. Either gas or gas mixed with hydrogen was used, an increase of NO_x was observed due to higher combustion temperatures obtained with increase of the equivalence ratio. Addition of hydrogen reduced CO₂ concentration due to dilution of carbon in the gas-hydrogen mixture. Methane was more completely burned and total hydrocarbons were decreased for the gas-hydrogen fuel. Important, the laser spark plug was operated for long about 10 h without deterioration.

A significant body of research on LI of natural gas reciprocating engines has been carried out at Argonne National Laboratory, USA. Early tests conducted at room temperature and in a static combustion chamber indicated that LI is useful at pressure levels beyond conventional ignition limits [111]. From experiments conducted in a rapid compression machine, operated at ~ 500 °C and up to 70 bar, it was shown that the lean limit for ignition can be extended up to the lean-flammability limit. Tests on a single-cylinder engine showed a reduction in NO_x emissions of up to 70% and efficiency improvement up to 3% in comparison with the classical ignition. The performances of a 6-cylinder natural gas engine ignited by laser were reported by Gupta et al. [112]. Fiber delivery was investigated as a solution to transmit the beam from a single laser head to the engine by multiplexing. However, the tests also indicated that available fibers were not practical due to reduced damage threshold, bending losses or a limited lifetime. A free-space transmission system for the laser beams was therefore preferred. LI of a Cummins QSK19G natural-gas engine demonstrated an extension of the air-fuel lean limit to $\lambda = 1.76$ from the 1.68 value determined for ignition by classical spark plugs. The performances of a single-cylinder natural gas engine (1.8 liters), ignited by a micro-laser ignition system developed by Denso Co., were reported by M. Biruduganti et al [113]. This passively Q-switched Nd:YAG/Cr⁴⁺:YAG ceramic laser delivered a train of up to 11 pulses at 1064 nm with 2.5 mJ pulse energy; water cooling was necessary to maintain good stability of laser operation. The brake thermal efficiency was significantly improved and the air-fuel lean limit extended up to $\lambda = 1.7$; whereas, a slight penalty in NO_x emission was observed. In another experiment an air-cooled, end-pumped, passively Q-switched Nd:YAG-Cr⁴⁺:YAG laser (1064 nm wavelength, 21 mJ per pulse energy, 4.2 ns duration) was used to ignite one cylinder of a turbocharged 6-cylinder natural-gas fueled engine [114]. LI extended the lean operation and improved the engine efficiency by 0.2% in comparison with electric spark ignition. The performances of a 6-cylinder lean-burn natural gas engine (Cummins QSK19G) that was operated only with laser igniters (one laser spark on each cylinder) were discussed by Gupta et al. [115]. The laser spark plug consisted of a Nd:YAG/Cr⁴⁺:YAG monolithic laser that was end pumped with high-power VCSEL; the laser delivered up to three-consecutive pulses, each with 14.5 mJ–16.5 mJ energy and 4.7 ns duration. An increase of efficiency by 1.47% was observed for LI with two pulses, a result that was attributed to improved ignition stability under advanced ignition timing conditions. Almansour et al. [116] has presented data recorded on a single-cylinder reciprocating natural gas engine, ignited with three different devices: a classical spark plug, LI and a pre-chamber LI system. The engine was operated at 1800 rpm speed and 10 bar BMEP load with various λ and at

different ignition timings. Whereas ignition by classical spark plug was optimum at $\lambda = 1.58$, pre-chamber LI extended the lean ignition limit up to $\lambda = 1.7$. An improvement of 2.1% in overall engine efficiency was measured for pre-chamber LI. Differences in CO and unburned hydrocarbon emissions were negligible for all three ignition systems. A conclusion was that pre-chamber LI could be a potential strategy to investigate to obtain improved efficiency from such an engine. As a comment, the results obtained in the field of LI of reciprocating natural gas engines are numerous and of impressive quality and importance; a review paper should be dedicated separately to these data, in the opinion of the authors.

Developments in the field of LI for aerospace and satellite use are also noticeable. Solid propellants of small-satellite propulsion systems can be ignited by low (around 1.0 W) power diode lasers [117]. The advantages of LI for space propulsion systems were highlighted in several talks given by Manfletti and Börner [118,119]; new designs are required for the transportation systems and LI is seen as an alternative technique to the existing ones. Minimum laser pulse energy for LI of CH_4/O_2 and H_2/O_2 propellants was evaluated by Börner et al. [120] and compared for two concepts of injection and two locations of ignition. A discussion on laser specifications for reliable ignition of gaseous and liquid fuels in gas turbine was given by Griffiths et al. [121]. The analysis included the optical configuration, characteristics of the laser pulse as well as properties of air-fuel mixtures. It was concluded that laser beam intensities higher than $3 \times 10^{13} \text{ W/cm}^2$ are required for LI of 15 MW industrial gas turbines. A ns LI system developed for ignition of aeronautic combustion engines was described recently by Amiard-Hudebine et al. [122]. The design was based on a microchip laser that yielded μJ energy, ns duration pulses that were then amplified in two successive amplifiers. The system was able to generate output pulses of 11 mJ energy with 1 ns duration at repetition rate 10 Hz. In addition, successful ignition of an experimental combustion chamber was achieved with this laser system. Of importance, an overview of advanced ignition techniques with an emphasis on LI and applications to aerospace propulsion was recently published by O'Briant et al. [123]. Laser ablation is envisaged to be essential for ignition of future rocket or other systems with new design. This includes thrusters for orbit correction (which need only mW-power level) as well as powerful GW-level systems used for launching into orbit.

It can be stated with a reasonable degree of certainty that LI has reached a quite good level of maturity with respect to its application in 'real world' engines. Gasoline automobile engines were run only by laser spark plugs, natural gas reciprocating engines with 6-cylinders were operated with such laser devices and significant steps were made towards LI of transportation systems for satellites. On the other hand, the interest and involvement of automotive firms and engine makers in this research area appear not to have grown or been sustained, at least not according to some expectations. Plausible reasons for this are that: the system price (per laser spark plug) is still high, further technical issues need to be solved or efforts need to be made to implement such an ignition system. It is possible that observed improvements in engine efficiency are not as expected and therefore do not yet justify large-scale application of LI, but it is also clear that LI is one of a number of technologies for potentially improving engine efficiency and reducing emissions that automotive companies are (or have been) considering.

4. Characterization of the laser ignition process

The potential of LI to improve the combustion characteristics of a reciprocating engine compared to conventional ignition has also been shown by other research groups, too. For example, Srivastava and Agarwal [124] have compared LI with conventional ignition of a single cylinder engine. They demonstrated a higher maximum combustion pressure, an earlier pressure rise and an increased heat release rate for the case of LI. In another study, the same authors have shown that LI additionally reduces the cyclic variations [125]. Yamaguchi et al. [126] have investigated two-point LI with a naturally aspirated gas engine. Here, it was shown that multipoint ignition improves the lean limit and the thermal efficiency. Cheng et al. [127] also used temporal multi-pulses to improve the performance and stability of a GDI engine. There, a second laser pulse was delivered at an appropriate time to stabilize and advance the combustion process. All these studies show that LI is able to improve the engine efficiency and reduce cyclic variations while, at the same time, reduce pollutant emissions. However, to exploit the full potential of LI, the mechanisms and the characteristics of the ignition process have to be understood.

4.1. Laser ignition process

The LI process, which will be discussed here, can be initiated by different mechanisms. In particular, the mechanisms can be divided into laser thermal ignition, laser induced photochemical ignition, laser induced resonant breakdown ignition and laser induced non-resonant breakdown ignition [7,17,24]. The most common LI mechanism used for ignition of a fuel/air-mixture is non-resonant breakdown.

The individual steps of the LI process via laser-induced non-resonant breakdown are illustrated in Fig. 12. A high peak power laser pulse is focused to generate plasma and to ignite a fuel/air mixture (Fig. 12a). The mechanism starts with the generation of free electrons by multi-photon ionization. Therefore, a sufficient number of photons has to be absorbed by an atom or a molecule, which in total provide the required ionization energy. This is very unlikely, since the ionization energy of gaseous oxygen and gaseous methane is in the order of 12 eV [23]. Using a Nd:YAG laser with the fundamental wavelength of 1064 nm and thus a single photon energy of 1.17 eV, more than 10 photons are required for ionization. Impurities in the gas mixture, like aerosols, dust or vapor can significantly reduce the ionization potential (<1 eV) [23]. Thus, the generation of initial electrons is attributed to impurities in the gas mixture [12,128–130]. The initial electrons gain their energy by absorbing more photons via the inverse bremsstrahlung process. Cascade ionization takes place if the initial electrons gain sufficient energy and ionize other gas molecules. This leads to a breakdown of the gas [131,132]. The induced plasma consists of highly reactive species that serve as the chemical source for ignition. If the plasma has sufficient energy, the ignition of an ignitable mixture can be initiated. The plasma breakdown is followed by detonation-like plasma propagation. The surrounding gas

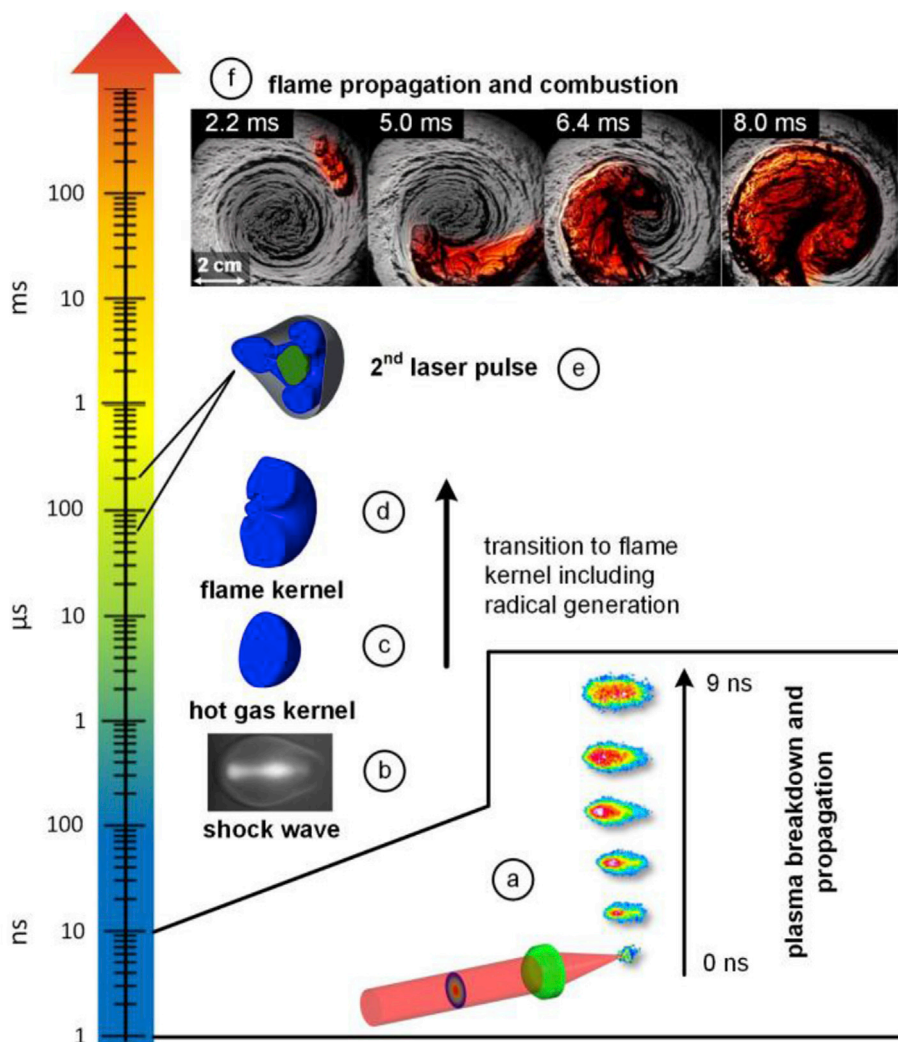


Fig. 12. Temporal progress of the LI process.

of the plasma is ionized. The dominant process in this phase is the interaction between the laser photons and the laser-supported detonation wave [15,17]. This leads to a more effective absorption of the laser radiation towards the laser direction and an increase of the plasma volume [133]. An energy transfer from the laser to the plasma takes place. Due to the laser supported detonation wave, the plasma propagates primarily towards the laser beam direction (Fig. 12a).

A shockwave (Fig. 12b) is released by the plasma caused by the rapid temperature and pressure rise after some tenth or hundreds of nanoseconds [16,17,134]. The shockwave propagates with supersonic speed into the cooler ambient gas [134]. The remaining hot gas is formed to a spherical hot gas kernel (Fig. 12c) which collapses after a few microseconds [135]. A donut-like structure with a so-called ‘third lobe’ (Fig. 12d) is formed due to gas dynamic effects after a few tenths of microseconds [16]. In the case of an ignitable mixture, a self-sustaining chemical reaction starts after 10 μs –50 μs [136–138]. Consequently, the hot gas kernel becomes a flame kernel during the formation of the third lobe. If pulse trains are used to ignite a fuel/air-mixture, the flame kernels of consecutive laser pulses interact with previously induced flame kernels [101]. Using a passively Q-switched laser, pulse trains with a temporal pulse spacing of 60 μs –250 μs can be applied. The interaction of a second flame kernel with the previous one is shown in Fig. 12e. The second flame kernel is formed in the center of the first flame kernel. The shockwave induced by the second breakdown propagates faster within the first flame kernel due to the lower density of the hot gas. The interaction between the flame kernels of a pulse train strongly depends on the flow velocity [101]. In the case of successful ignition, sustained flame propagation (Fig. 12e) leads to the complete combustion of the fuel air mixture.

In the following sections, a review of measurement techniques to analyze the early LI process is presented. The review deals with the following individual steps of the ignition process: a) Energy transfer from laser to plasma; b) Plasma development and evolution; c) Shock wave propagation, and d) Flame kernel development and propagation.

4.2. Energy transfer from laser to plasma

The energy transfer from laser to plasma is the first step after the optical breakdown of the laser ignition process. The laser energy absorbed by the plasma (E_{abs}) can be calculated by the following simple equation:

$$E_{abs} = E_{laser} - E_{trans} - E_{scattered} \quad (1)$$

where, E_{laser} is the incident laser energy, E_{trans} represents the transmitted laser energy and $E_{scattered}$ denotes the laser energy scattered by the plasma. In most investigations plasma scattering is neglected [32,106,107,139–143]. Schwarz et al. [144] suggested an experimental setup to measure the scattered laser energy after a laser induced breakdown. They induced plasma generation within an integrated sphere and measured the scattered laser energy with a photodiode. Such an experimental setup is depicted in Fig. 13.

The results of Schwarz et al. [144] show that the amount of the scattered laser energy is less than 3% at an incident laser energy of 10 mJ (at 1064-nm wavelength). The energy loss due to the delayed optical breakdown (E_{trans}) is much higher than by plasma scattering. This demonstrates that plasma scattering can be neglected in Eq. (1). A simple and common technique to analyze the transferred energy from the laser pulse to plasma is to measure the laser energy before and after the plasma. The absorbed energy can be calculated by subtracting the transferred laser energy from the incident laser energy. This measurement technique does not consider plasma scattering. An experimental setup of this method is shown in Fig. 14. The incident laser energy can be measured by applying either a beam splitter or a mirror. Using the latter method the incident and transferred laser energy cannot be measured simultaneously. The described technique is used by many researchers to measure the absorbed laser energy [11,139,140,142–147]. In these studies, the amount of the absorbed laser energy typically shows up in the range of 50%–80% mainly depending on the incident laser energy, the focal length of the lens and the ambient pressure. This demonstrates that laser transmission and absorption play a more important role than plasma scattering.

The recent development of LI systems has been reported in the previous section, where we showed that passively Q-switched laser (PQL) ignition systems have considerable potential as a future ignition source. PQLs can emit pulse trains of several pulses by increasing the pump power, with the temporal spacing of the individual pulses being adjustable between a few tenths of microseconds and a few hundred microseconds. Moreover, a partially saturated absorber exhibits a complex spatial transmission [148] that can lead to a complex temporal and spatial energy distribution [106]. The energy transfer measurement technique described earlier does not consider such a property. A power or energy meter measures the energy or the average power. Such devices do not provide information about the temporal and spatial energy distribution of the laser pulse. However, the complex pulse profile of PQL is decisive for the energy transfer after an optical breakdown. Additionally, LI system components (laser spark plugs, laser active medium, lenses) are often sealed in their mountings, making measurements of the incident laser energy unfeasible. Furthermore, the analysis of the individual pulses of a pulse train is not possible with a common laser energy or power meter.

Lorenz et al. [106] therefore introduced an alternative measurement technique to analyze the energy transfer from laser to plasma, which considers the special specifications of PQL spark plugs. The technique is based on the detection of temporal pulse profiles and analysis of the temporal and spatial energy distribution, with and without optical breakdown. Analysis of the pulse profile without an optical breakdown is realized by testing in a vacuum chamber. Also, the individual pulses of a pulse train can be detected by this measurement technique. The experimental setup can be seen in Fig. 15.

The laser spark plug is mounted in an optically accessible vacuum pressure chamber. The focal point of the sealed spark plugs is positioned centrally in the chamber. A lens outside of the chamber collimates the laser beam before it passes through a filter box and is converged again to enter the detection box. The detection box consists of diffusers, a band pass filter transmitting the laser light and a fast pin-photodiode connected to a digital storage oscilloscope. The energy of the individual pulses can be determined from the recorded pulse profiles. For measurement of the pulse energy delivered by the laser spark plug, the chamber is evacuated by a vacuum pump. At increased pressures, the influence of elevated gas densities on the energy transfer can be examined [106]. As mentioned previously, the measurement technique distinguishes between the global energy transfer (based on the temporal pulse profile) and the local energy transfer (based on the temporal and spatial pulse profile). To examine the local energy transfer, spatial filters are placed in the filter box. Thus, different ring areas of the laser pulse profile can be detected [106].

Results of these measurements published by Lorenz et al. [106] demonstrate that the center part of the passively Q-switched laser

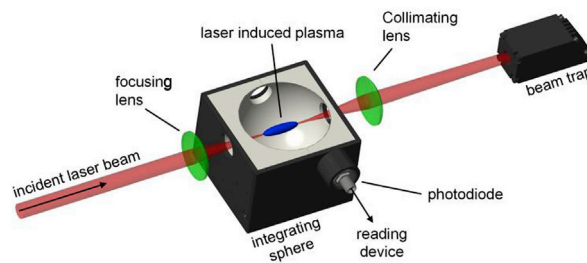


Fig. 13. Experimental setup to measure the scattered laser light by the plasma.

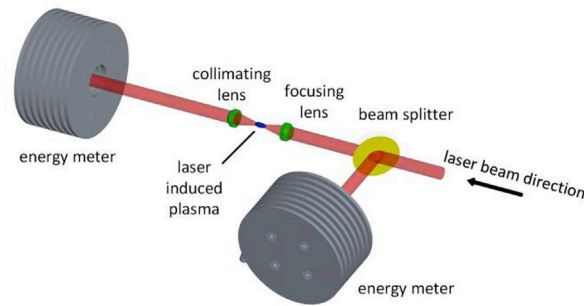


Fig. 14. Experimental setup to measure the energy transferred from laser to plasma.

pulse is emitted earlier than the outer parts (Fig. 16). Moreover, it can be seen that the highest power density is reached in the center of the laser pulse. The arrows in Fig. 16 indicate the time of the breakdown at different ambient pressures. Plasma breakdown is induced by the center part of the laser pulse and occurs before the largest part of the outer ring areas arrives at the focal point. Optically dense plasma is already developed at the time of the emission of the outer parts of the laser pulse. Thus, these parts are effectively absorbed by the plasma [101,106].

4.3. Plasma development and evolution

The second step of the LI process is the plasma development and evolution. This step links the energy transfer with the flame kernel formation. Different measurement techniques to characterize the plasma development and evolution are available. These include two-frame shadowgraphy [134], Langmuir probe [149], Thomson scattering [150,151], laser interferometry [152–155], plasma spectroscopy [101,156–161] and plasma imaging [107,139,147,158–160,162–166]. The following section deals with the most relevant methods, those being plasma imaging and laser induced breakdown spectroscopy (LIBS).

4.3.1. Plasma imaging

A common method used to acquire the plasma propagation is plasma imaging [107,139,147,158–160,162–166]. The general setup of such an experiment is depicted in Fig. 17. The spontaneous emission of the laser induced plasma is focused on a camera with a lens system. The plasma evolution is a rapid process; therefore, a camera with a short exposure time in the nanosecond timescale is necessary. An appropriate shutter speed provides an intensified CCD camera. In the case of LI with an actively Q-switched laser, the camera trigger and the trigger of the Q-switch can be synchronized. In the case of a passively Q-switched laser, however, the SA is bleached by the laser emission, resulting in an inevitable temporal jitter of a few microseconds of the emitted laser pulse. Thus, laser pulse emission and camera exposure cannot be harmonized. A possibility to synchronize the laser pulse and the camera system is to trigger the camera by the laser pulse itself. Therefore, the laser pulse is transformed into an electrical trigger signal by a fast photodiode (Fig. 17). This method leads to a minimum delay between laser pulse emission and recording time of a few tenths of microseconds [107].

An alternative triggering method to achieve plasma recordings immediately after the breakdown from a passively Q-switched laser was introduced by Bärwinkel et al. [107]. The pump laser and the camera are triggered with a fixed delay between each other. A digital storage oscilloscope records the electrical trigger signal of the fast photodiode and the monitor signal of the camera. This trigger method allows plasma images even during the laser pulse emission. The temporal dependency of optical breakdown in air induced by a passively Q-switched laser and the spontaneous plasma emission are shown at the top of Fig. 18. The black lines correspond to laser pulse profiles either with (solid line) and without (dashed line) optical breakdown. The orange line indicates the profile of the spontaneous plasma emission. A laser pulse with energy 6.2 mJ is applied here. The plasma emission starts shortly after the optical breakdown, indicated by the fast falling edge in the laser pulse profile, and reaches its maximum intensity near the end of the laser pulse emission. Plasma images taken during (A–D) and after the laser pulse emission (E–H) are shown at the bottom of Fig. 18. Images A–E are recorded with the trigger method with a fixed delay between pump laser and camera [107] and for images F–H the camera is triggered by the laser pulse itself. The images B–D indicate that the plasma propagates during the laser pulse emission towards the laser beam direction. This is attributed to the laser supported detonation wave [107]. After the laser pulse emission, the plasma propagates in all directions equally (images F–H), since there is no longer energy supplied to the plasma.

4.3.2. Laser induced breakdown spectroscopy

Spectroscopic analysis is a common and convenient technique to characterize laser induced plasma [101,156–161]. Besides elementary analysis, the electron density and plasma temperature can also be investigated. In this section, we discuss the determination of the plasma temperature, which is a crucial factor in early flame kernel development.

The plasma temperature is calculated from spectra of the spontaneous plasma emission. The measurement system consists of a spectrometer and a suitable (ICCD) camera recording the dispersed plasma radiation. Both trigger methods described in the previous section can be applied. The term plasma temperature denotes the electron excitation temperature. To obtain reliable and quantitative

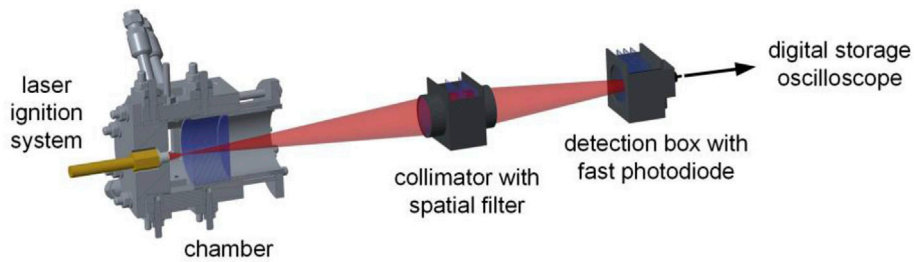


Fig. 15. Experimental setup for measuring the temporal and spatial energy distribution of a LI system.

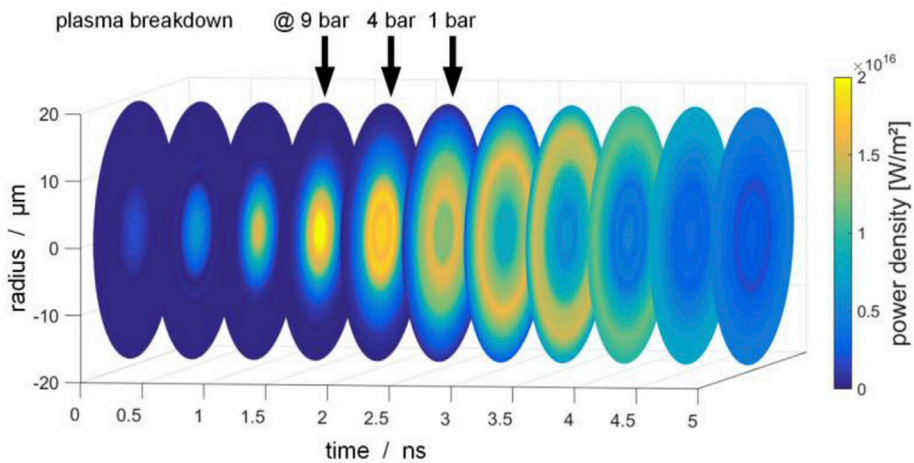


Fig. 16. Temporal and spatial energy distribution within the transmitted profile of a 12.3 mJ PQL without breakdown (calculated from data of Lorenz et al. [106]).

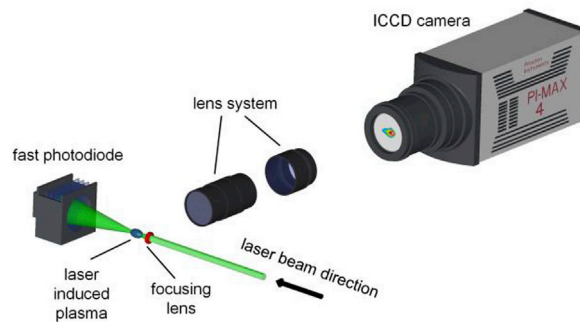


Fig. 17. Experimental setup for plasma imaging using a passively Q-switched ignition laser.

results from LIBS measurements, the plasma has to reach a state of local thermal equilibrium (LTE). This can be assumed if at least one of the following criteria is met [156]:

- The EEDF Maxwell criterion requires that the electron density $N_e > 10^{16} \text{ cm}^{-3}$ and $kT < 5 \text{ eV}$; k is the Boltzmann constant and T is the plasma temperature;
- The McWhirter criterion requires that $N_e > 1.6 \times 10^{12} T^{0.5} (\Delta E)$, where ΔE is the largest energy gap between the upper and lower energy states of spectroscopic lines used;
- All data points of the Boltzmann plot can be fitted to a straight line.

Several methods can be used to calculate the plasma temperature [156], the most common one used in LI research being the Boltzmann method [101,159,167,168]. A Boltzmann plot is generated from the area below the spectral lines and the corresponding data

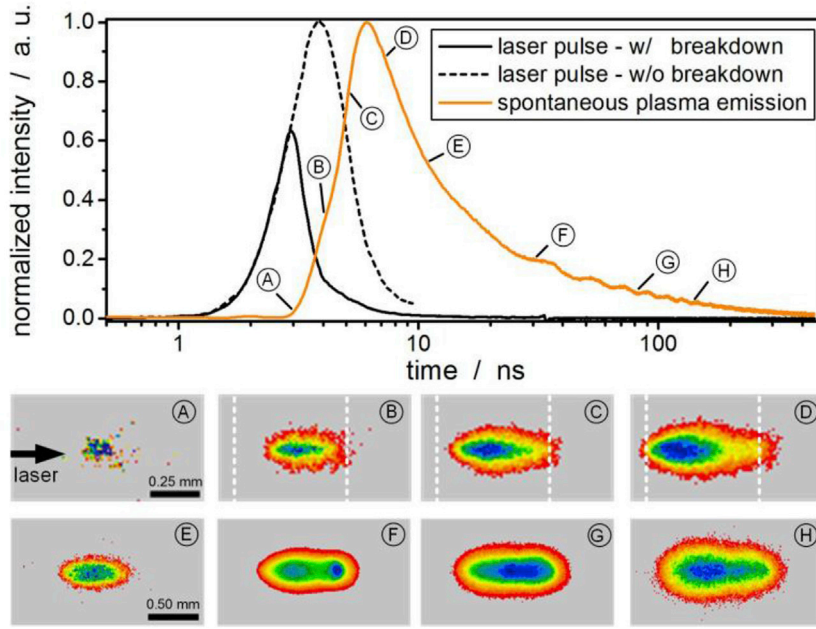


Fig. 18. Temporal laser pulse profiles of an unaffected and a focused laser pulse and corresponding images of spontaneous plasma emission (passively Q-switched laser, laser energy of 6.2 mJ, FWHM of 2.6 ns).

transitions. The spectral lines can be obtained by applying a multi-pulse fit to the recorded spectra [101]. The Boltzmann relation for emissivity of the spectral transition is given by Zhang et al. [156]:

$$\frac{\epsilon_{nm}\lambda_{nm}}{A_{nm}g_n} = \frac{hcN}{4\pi U(T)} e^{-\frac{E_n}{kT}} \quad (2)$$

where the subscripts n and m signify the upper and the lower excited levels of a species, ϵ_{nm} is the emissivity, λ_{nm} the wavelength of the transition, A_{nm} the transition possibility and g_n the degeneracy of the upper level of the transition. N describes the number density of the species, h the Planck constant, c the speed of light and $U(T)$ the partition function, where T is the excitation temperature. E_n represents the energy of the upper state and k the Boltzmann constant. Assuming an optically thin plasma, the emissivity ϵ_{nm} can be substituted by the integrated intensity I_{nm} of the transition in Eq. (2) [169]. Taking the logarithm and substituting ϵ_{nm} with I_{nm} , Eq. (2) can be rewritten as follows [156]:

$$\ln\left(\frac{I_{nm}\lambda_{nm}}{A_{nm}g_n}\right) = -\frac{E_n}{kT} + \ln\left(\frac{hcN}{U(T)}\right) \quad (3)$$

The plasma temperature can be obtained by plotting the value $\ln[(I_{nm}\lambda_{nm})/(A_{nm}g_n)]$ versus the upper state energy E_n . The data points form a straight line and the plasma temperature can be calculated by the equation [156]:

$$T = -\frac{1}{kb} \quad (4)$$

where b is the slope of the fitted straight line. With this expression, the plasma temperature can be calculated without knowing the value of the partition function $U(T)$. In order to apply this method, at least two spectral data points are necessary. However, the accuracy of the calculated temperature can be improved by considering more than two spectral lines [156].

Fig. 19 compares the results from different investigations [101,158,159,168] into the temporal temperature profile of a laser-induced plasma. The experimental conditions used in these studies are summarized in Table 3. Lorenz et al. [101] evaluated the plasma temperature to within 10 ns of the optical breakdown. The measurement system used both methods of triggering described in the previous section. The plasma temperature was observed to decrease continuously with the time, the temperature profile having a strong gradient in the first few nanoseconds, though less pronounced at later times. The calculated temperatures in this study ranged between the values observed by Glumac et al. [158] and Harilal [168]. However, the qualitative progression was comparable. Lorenz et al. [101] and Harilal [168] applied the Boltzmann method to calculate the plasma temperature. In contrast, Glumac et al. [158] used an alternative evaluation called the synthetic spectra method. The temperatures calculated by Kawahara et al. [159] are well above the temperatures calculated in the other studies in the first 200 ns. Kawahara et al. [159] have used the Boltzmann two-line method for the temperature evaluation. Using only two lines for the analysis may lead to these differences. In general, the accuracy of the temperature calculation using the Boltzmann method is only as good as the linearity of the Boltzmann plot.

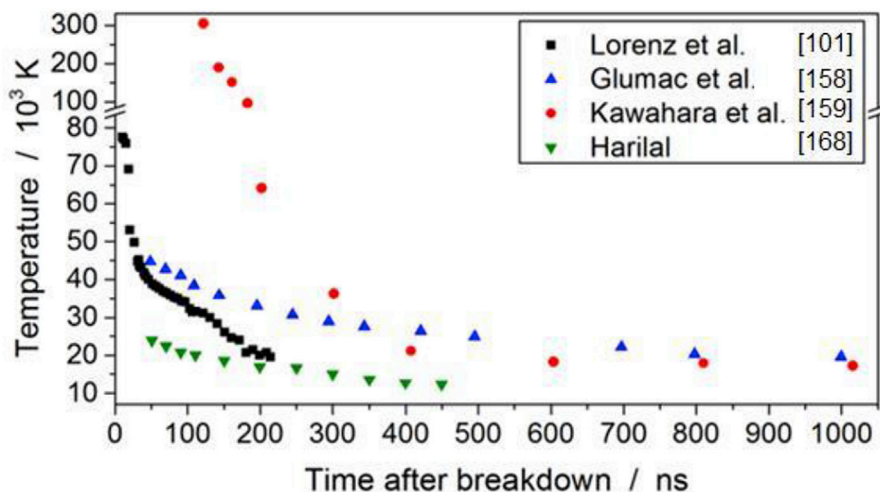


Fig. 19. Comparison of plasma temperature calculations from different studies.

Table 3

Experimental conditions for the referred studies given in Fig. 19.

Author/Reference	Atmosphere	Laser pulse energy, E_p (mJ)	Wavelength, λ (nm)	Pulse duration (nm)	Focal lens, f (mm)
Lorenz et al. [101]	Air	~10	1064	0.5–3	N/A
Glumac et al. [158]	Air	180	532	6.8	100
Kawahara et al. [159]	Air	170	532	8	200
Harilal [168]	Argon	100	532	8	75

Lorenz and Brüggemann [170] have investigated the spatial temperature distribution of laser-induced plasma in argon by one-dimensional spectroscopy. Experiments were performed with two lasers of different temporal pulse shapes. They observed different spatial temperature gradients towards the laser beam direction, due to the different laser pulse shapes. The spatial plasma distribution has a direct impact on flame kernel formation (section 4.4).

4.3.3. Shock wave propagation

The laser-induced plasma releases a shock wave in the first few hundreds of nanoseconds due to the high temperature and pressure difference in relation to the surrounding gas [16,17]. Since the supersonic propagation of the shock wave [134] is a transparent phenomenon, an appropriate measurement technique has to be found. Rayleigh scattering [163] or the beam deflection method [15,171] were examined to explore the shock wave evolution. However, the high-speed shadowgraphy [135,152,157,172,173] and high-speed Schlieren measurement technique [99,142,174–176] is often applied and easy to implement. These techniques are briefly introduced in this section.

The shadowgraphy and the Schlieren technique are closely linked. Both methods can visualize the transparent phenomenon 'Schlieren'. Schlieren occur when an area in a medium is different in a physical property from the surrounding (i.e. temperature, pressure or concentration difference). The variation in the physical properties results in a change of the refractive index. Both techniques depict an integrated image of the evaluated object. A shadowgram is the image of an ordinary shadow whereas the Schlieren method records an optical image formed with lenses. Furthermore, a knife-edge or something similar is necessary to cutoff the refracted light rays. Such cutoff elements are not needed for shadowgraphy. Another difference is the experimental setup of the methods [177].

The experimental design of the shadowgraphy and the Schlieren methods are treated in the following. A simple setup of a shadowgraphy experiment is shown in Fig. 20a. A point light source is collimated by a lens and illuminates the test area with a dense spherical Schlieren object. The Schlieren object alone can be observed, if its refractive index is higher than the refractive index of the surrounding gas. Consequently, the spherical Schlieren object acts as a positive lens and can be imaged in the screen. An appropriate camera can substitute for the screen. The left part of the simple Schlieren setup equals the shadowgraphy alignment (Fig. 20b). The light of a point light source is collimated and is focused by a second lens. The Schlieren diffracts the parallel light ray, with the diffracted rays being partly cut-off by the knife-edge placed at the focus of the second lens. Thus, the Schlieren object appears darker on the screen than its environment. A pinhole aperture or an optical slit can be applied as a cutoff element instead of a knife-edge. The Schlieren measurement method is favorable in the case of weak disturbances, due to its higher sensitivity compared to shadowgraphy techniques [177].

Shock waves induced by a laser create strong variations in the refractive index of the ambient gas. Therefore, both Schlieren and shadowgraphy measurement techniques are appropriate tools to examine the shock wave propagation. A time series of the shock wave after a laser-induced breakdown in air is displayed in Fig. 21 (first row). The images are obtained by the high-speed Schlieren

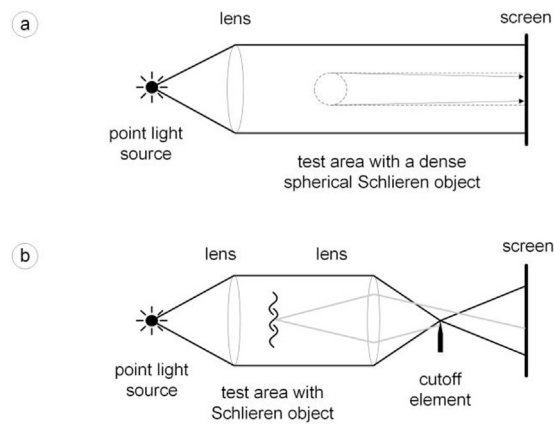


Fig. 20. a) Fundamental components of a shadowgraphy. b) A Schlieren measurement technique setup (according to [177]).

measurement technique. An emICCD camera (Princeton Instruments, PI-MAX 4) is applied to record the images. The exposure time was set to 50 ns (500 ns and 750 ns delay) and 100 ns (1000 ns - 2000 ns delay).

4.4. Flame kernel development

After the shock wave release, a flame kernel is formed from the remaining hot gas kernel. The flame kernel has a donut-like structure with a so called third lobe resulting from gas dynamic effects due to the shock wave and there from occurring refraction wave [15]. In case of an ignitable ambient gas, radicals are generated within the flame kernel. Only a sufficient number of radicals lead to a successful ignition [141].

Several measurement techniques have been explored to investigate the flame kernel development and propagation. A selection of techniques and the corresponding references are as follows: a) High-speed-Schlieren measurement technique [11,16,101,103,138,142,178–181]; b) CH^* -chemiluminescence [143,182]; c) Planar laser induced fluorescence [136–138,183,184] and d) Rayleigh scattering [160,185–187].

4.4.1. High-speed Schlieren technique

The high-speed Schlieren method is a common and often applied measurement technique for investigations of the flame kernel development. The experimental setup is similar to the setup for the shock wave examination and is described in the previous section (Fig. 20b). The shadowgraphy method is not suitable for studies on the flame kernel because the variation of the refractive index within the flame kernel structure is weak.

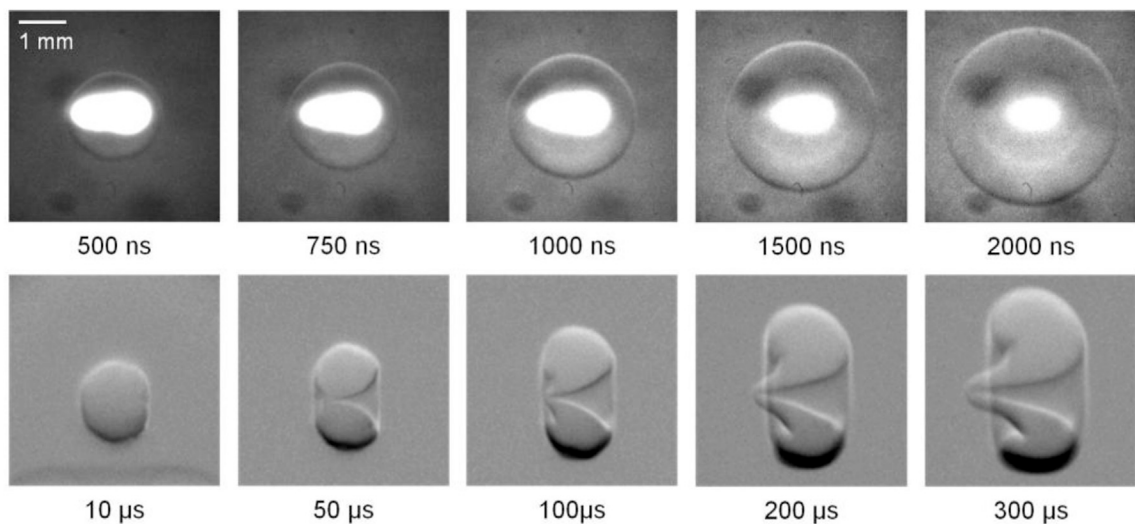


Fig. 21. Time series of Schlieren images of the shock wave (quiescent air) and the flame kernel (methane/air-flow, $v = 1$ m/s; $\lambda = 1.2$) after laser-induced breakdown (laser energy of 6.2 mJ, FWHM of 2.6 ns).

An example of flame kernel propagation observed by the high-speed Schlieren technique is depicted in Fig. 21 (second row). For acquisition of the images, a high-speed camera (Photron, Fastcam SA-X2) is applied. A lean methane/air-flow ($\lambda = 1.2$) is ignited at ambient pressure. The influence of the flow on the flame kernel development is minimized by adjusting the flow velocity to 1 m/s. The initial flame kernel (10 μs) has a spherical structure. The above-mentioned gas dynamic effect forms toroidal vortex flows on the laser facing and averted side of the initial flame kernel. This leads to the donut-like structure (50 μs). The vortex on the laser-averted side is stronger and thus, the third lobe is developed (200 μs). The dominating vortex is determined by the spatial plasma temperature distribution [16,180].

4.4.2. CH^* flame chemiluminescence

Bak et al. [143,182] used the CH^* flame chemiluminescence to visualize the flame kernel structure after laser ignition of an ethane/air-flow and premixed methane/air mixtures. The chemiluminescence signal is filtered by a band-pass filter (430 nm, bandwidth 10 nm) and recorded by an ICCD camera.

4.4.3. Planar laser-induced fluorescence

The Schlieren method as well as the CH^* flame chemiluminescence are integrating techniques. Planar laser induced fluorescence (pLIF) enables the recording of cross-sectional images and the detection of minor species of a combustion process. Thus, the flame front location is precisely visualized with a high spatial resolution by detecting combustion radicals, i.e. the OH or C_xH_y radical [188]. The minor species are exposed with laser radiation of a species-specific wavelength (usually in the UV) leading to a transition to an excited electronic state of the radicals. When this excited state decays, photons with a red shifted wavelength compared to the excitation wavelength are emitted.

In the case of investigation of the flame kernel after LI, an excitation laser beam is formed into a light sheet to illuminate a layer within the flame kernel. The fluorescence signal is detected perpendicular to the light sheet with an ICCD camera. Of course, appropriate filters are applied, thus transmitting only the desired fluorescence signal. Rayleigh scattering and other fluorescence signals are filtered. A schematic experimental setup of the planar laser induced fluorescence is shown in Fig. 22.

LIF enables absolute values of density and temperature distribution within the measured volume to be obtained. However, the determination of these values is difficult due to inhibiting effects on the detected fluorescence signal such as collision quenching, photoionization and pre-dissociation [189]. The major impeding factor is collision quenching. Here, the excited state may transition radiationless to the ground state by collisions [190]. The quenching rate depends on the state, the collision rate and on the collider itself [138]. Therefore, in most studies regarding laser ignition [137,138,183,184]. Planar LIF (PLIF) is used to determine the qualitative densities of the observed species and to obtain time resolved cross-sections of the laser induced flame kernel. Chen and Lewis [137] applied PLIF to visualize the flame kernel after laser ignition of a NH_3/O_2 mixture. In addition, the temperature and the NH density is calculated from the PLIF images. Maximum temperatures of about 3300 K and 2400 K were found after 3.3 μs and 20.3 μs , respectively.

4.4.4. Rayleigh scattering

The Rayleigh scattering method uses the elastic scattering of photons of a probe laser from the molecules of the investigated gas. The Rayleigh signal is proportional to the total number density. If the assumption of a constant pressure and the application of the ideal gas law are reasonable, the temperature is inversely proportional to the detected Rayleigh signal. An accurate determination of the temperature is only possible, if the chemical composition of the gas and the Rayleigh cross-section is known. Alternatively, reference measurements of the gas with known temperature and cross-section may be used to validate the Rayleigh scattering technique [190,191]. The Rayleigh signal is independent of the wavelength, since the Rayleigh scattering is an elastic scattering. Thus, the probe laser can be chosen freely. However, the $1/\lambda^4$ -dependency of the Rayleigh cross-section leads to an increasing Rayleigh signal by

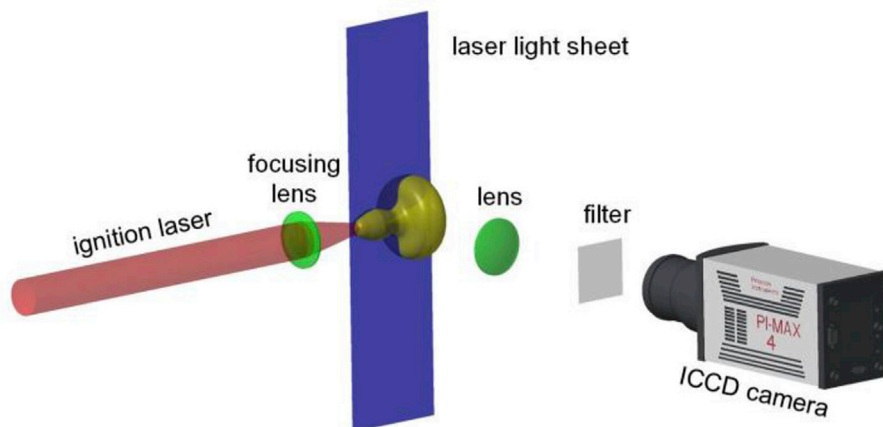


Fig. 22. Experimental Setup of the planar laser induced fluorescence.

decreasing the wavelength of the probe laser [190].

The freedom of choice of the excitation wavelength and the relative simple experimental setup makes the Rayleigh scattering technique attractive. However, Rayleigh scattering is not sensitive to certain species. Furthermore, superimposing the Rayleigh signal with background scattered light can distort the measurements. Background scattering is caused by walls and windows of the combustion chamber or entrained particles. The influence of the background scattering can be suppressed, for example, by applying the filtered Rayleigh scattering (FRS) technique [190–192].

To determine the spatial temperature distribution within the flame kernel, the probe laser beam has to be formed to a light sheet to obtain a two-dimensional measurement signal. The experimental setup of the Rayleigh scattering technique is quite similar to the setup of the PLIF technique (Fig. 22). The light sheet crosses the focal point of the laser beam desired to induce the plasma for ignition. An ICCD camera perpendicular to the light sheet detects the scattered light. Appropriate filters have to be chosen to inhibit the detection of fluorescence or the background scattering in case of FRS.

Nassif and Hüwel [186] have applied the Rayleigh scattering technique to determine the temperature distribution within the flame kernel, using a diode array to detect the scattered light. The influence of the background light scattered by the walls on the detected signal was minimized by polarizing the probe laser. Temperature distributions for delays from 30 μs to 2000 μs after the breakdown were established. The calculated temperatures ranges from 4500 K at 30 μs to 350 K at 2000 μs after the plasma breakdown (ignition laser energy 250 mJ). Glumac et al. [158] have measured the spatial temperature distribution of the flame kernel, with the filtered Rayleigh scattering technique being used to eliminate background scattering. The laser spark was generated in air by a frequency-doubled Nd:YAG laser with pulse energy 180 mJ. Temperatures between approximately 4100 K (20 μs after breakdown) and 580 K (1000 μs after breakdown) appear in the flame kernel. It should be mentioned that both of these aforementioned studies were performed in non-flammable atmospheres. However, the Rayleigh scattering method can also be applied to combustion environments [183,192].

The above results demonstrate that the LI process can be readily examined by optical measurement techniques. Different phenomena are involved in each stage of the ignition process and therefore an appropriate method has to be selected to investigate the different aspects. New insights into the LI process can be gained by applying optical measurement techniques adapted to the specific phenomenon. The acquired knowledge can be meaningful for engine developers to improve the ignition as well as the combustion, and in consequence the engine efficiency.

5. Conclusions

In comparison with classical ignition by the electrical spark plug, LI brings several potential advantages that cannot be ignored and that are interesting from both research and practical points of view. The flame kernel is not quenched, thus opening the possibility to improve the engine efficiency. The laser beam can, in principle, be focused at any position (even multiple positions) in the engine cylinder, enabling further engine design to be proposed. Temporal control of ignition (including multi-pulse) as well as spatial control (multi-point ignition) are applicable and can be exploited for engine operation with lean air-fuel mixtures or at high pressures. Results on LI were reviewed in this work, showing that important steps have been taken recently to put this method of ignition into practice.

The transfer through an optical fiber of the beam from a laser source placed remotely to the engine cylinder was also discussed. However, at the time of reporting here, the results obtained from this particular approach are not conclusive. Although the simplicity and flexibility of such a method and system are attractive as a concept, scientific and technological issues associated with the development of optical fibers of high-damage threshold remain a research challenge.

A second approach, of positioning the laser spark plug(s) directly on the engine cylinder and transporting the pump beam from a remote source to the laser spark plug, seems the most attractive one to follow for LI, especially for automobile engine and natural gas reciprocating engines, or space applications. This approach was envisaged before 2005 by a research team from the Technical University of Vienna in Austria, with the research targeting realization of rugged, compact lasers that could be mounted directly on the engine (simply retrofitting for the classical spark plug). Development of such lasers that are capable of operation in adverse conditions of vibration and temperature is challenging. Nevertheless, at this time, several laser spark-plug igniters have been realized. All solutions concluded that the optimum choice for the laser medium is a composite Nd:YAG/Cr⁴⁺:YAG structure (single crystal or all-poly-crystalline) with monolithic laser oscillator. Diode lasers (fiber coupled or array), arranged either in longitudinal- or side-pumping schemes, appear to be the most popular sources for exciting the Nd:YAG/Cr⁴⁺:YAG medium. VCSELs have also been shown to be a promising pump source in an end-pumping configuration, due to a less influence of temperature on its output performance (especially with regard to the emitting wavelength).

As an accomplishment of these investigations, a car was propelled by LI (i.e. with laser spark plugs alone) for the first time in Japan; the report was made at the 1st Laser Ignition Conference, April 2013, Yokohama, Japan (LIC '13). The research was carried out by a team from the Institute for Molecular Science, Okazaki, in collaboration with the Denso Company. Improved stability of operation at 1200 rpm speed was determined for LI in comparison with ignition by conventional spark plugs. A second work performed in Romania (a collaboration between National Institute for Laser, Plasma and Radiation Physics, Magurele and Renault Technologies Roumanie) also succeeded in running a car entirely by laser spark plugs. The results were presented at the 5th edition of Laser Ignition Conference (LIC '17), Bucharest, in June 2017. Measurements of stability and exhaust emissions were also performed on a similar 4-cylinder engine mounted on a test bench. It was concluded that LI improved engine stability appreciably at low speed and moderate load, but less so at high speed and load. Decreases in CO and HC emissions were measured from the laser-ignited engine. In contrast, an increase in NO_x emission was determined for LI in comparison with ignition by classical spark plugs.

At Argonne National Laboratory, a laser spark plug pumped by fiber-coupled diode laser was used to run a single-cylinder natural gas engine. Furthermore, a 6-cylinder natural gas stationary engine was operated entirely with laser spark plugs, built with VCSELs as pump

sources. An increase in the engine efficiency (by $\sim 1.47\%$) was determined in the latter case for LI in comparison with classical spark plug ignition. Some more comments can be made. For example, the side-pumped HiPoLas[®] Nd:YAG laser (Carinthian Tech Research, Villach, Austria) seems to be an optimum device for ignition of rocket engines, as reported in several communications given at the LIC'17 conference. Compact lasers with multiple-beam output were also realized, but compactness and operation in adverse conditions are issues that need further attention. Very few studies were dealing with the optimization of the window placed between the laser spark plug and the engine cylinder.

It is believed that although the technology has reached a degree of maturity enough to provide laser ignition as an alternative to classic ignition by spark plugs, the interest of automotive companies (mainly) will definitely put its mark on the future of laser ignition.

Acknowledgements

Financing: The European Union's Horizon 2020 Research and Innovation Programme, Grant agreement No 691688 (LASIG-TWIN); Ministry of Research and Innovation, Romania, CNCS - UEFISCDI, project number PN-III-P4-ID-PCE-2016-0332, within PNCDI III; German Research Foundation (DFG) under grant no. BR 1713/13-1.

References

- [1] P.D. Maker, R.W. Terhune, C.M. Savage, Optical third harmonic generation, in: 3rd Int. Conf. Quantum Elect., Paris, France, 1963, pp. 1559–1572.
- [2] J.H. Lee, R. Knystautas, Laser spark ignition of chemically reactive gases, *AIAA J.* 7 (2) (1969) 312–317.
- [3] F.J. Weinberg, J.R. Wilson, A preliminary investigation of the use of focused laser beams for minimum ignition energy studies, *Proc. Math. Phys. Eng. Sci.* 321 (1544) (1971) 41–52.
- [4] R. Hickling, W. Smith, Combustion Bomb Tests of Laser Ignition, SAE International, 1974, <http://dx.doi.org/10.4271/740114>. Paper 740114.
- [5] J.D. Dale, P.R. Smy, R.M. Clements, Laser Ignited Internal Combustion Engine: an Experimental Study, SAE International, 1978, <http://dx.doi.org/10.4271/780329>. Paper 780329.
- [6] J.D. Dale, P.R. Smy, The first laser ignition engine experiment (c.a. 1976), in: Laser Ignition Conference, OSA Technical Digest (Online), Optical Society of America, 2015 paper T3A.1.
- [7] P.D. Ronney, Laser versus conventional ignition of flames, *Opt. Eng.* 33 (2) (1994) 510–521.
- [8] J.X. Ma, D.R. Alexander, D.E. Poulain, Laser spark ignition and combustion characteristics of methane-air mixtures, *Combust. Flame* 112 (4) (1998) 492–506.
- [9] T.X. Phuoc, F.P. White, Laser-induced spark ignition of CH₄/air mixtures, *Combust. Flame* 119 (3) (1998) 203–216.
- [10] T.-W. Lee, V. Jain, S. Kozola, Measurements of minimum ignition energy by using laser sparks for hydrocarbon fuels in air: propane, dodecane, and jet-A fuel, *Combust. Flame* 125 (4) (2001) 1320–1328.
- [11] J.-L. Beduneau, B. Kim, L. Zimmer, Y. Ikeda, Measurements of minimum ignition energy in premixed laminar methane/air flow by using laser induced spark, *Combust. Flame* 132 (4) (2003) 653–665.
- [12] H. Kopecek, H. Maier, G. Reider, F. Winter, E. Wintner, Laser ignition of methane-air mixtures at high pressures, *Exp. Therm. Fluid Sci.* 27 (4) (2003) 499–503.
- [13] M. Weinrotter, H. Kopecek, M. Tesch, E. Wintner, M. Lackner, F. Winter, Laser ignition of ultra-lean methane/hydrogen/air mixtures at high temperature and pressure, *Exp. Therm. Fluid Sci.* 29 (5) (2005) 569–577.
- [14] M. Weinrotter, H. Kopecek, E. Wintner, M. Lackner, F. Winter, Application of laser ignition to hydrogen-air mixtures at high pressures, *Int. J. Hydrog. Energy* 30 (3) (2005) 319–326.
- [15] T.X. Phuoc, An experimental and numerical study of laser-induced spark in air, *Opt. Lasers Eng.* 43 (2) (2005) 113–129.
- [16] D. Bradley, C.G.W. Sheppard, I.M. Suardjaja, R. Woolley, Fundamentals of high-energy spark ignition with lasers, *Combust. Flame* 138 (1–2) (2004) 55–77.
- [17] T.X. Phuoc, Laser-induced spark ignition fundamental and applications, *Opt. Lasers Eng.* 44 (5) (2006) 351–397.
- [18] C. Xu, D. Fang, Q. Luo, J. Ma, Y. Xie, A comparative study of laser ignition and spark ignition with gasoline-air mixtures, *Opt. Laser Technol.* 64 (2014) 343–351.
- [19] G. Liedl, D. Schuocker, B. Geringer, J. Graf, D. Klavatsch, H. Lenz, W. Piock, M. Jetzinger, P. Kapus, Laser induced ignition of gasoline direct injection engines, in: *Proceed. SPIE*, vol. 5777, 2004, pp. 955–960.
- [20] T. Alger, D. Mehta, C. Chadwell, C. Roberts, Laser Ignition in a Pre-mixed Engine: the Effect of Focal Volume and Energy Density on Stability and the Lean Operating Limit, SAE Technical Paper, 2005, 2005-01-3752.
- [21] R. Dodd, J. Mullett, S. Carroll, G. Dearden, A.T. Shenton, K.G. Watkins, G. Triantos, S. Keen, Laser ignition of an IC test engine using an Nd:YAG laser and the effect of key laser parameters on engine combustion performance, *Laser Eng.* 17 (2007) 213–231.
- [22] J.D. Mullett, P.B. Dickinson, A.T. Shenton, G. Dearden, K.G. Watkins, Multi-cylinder Laser and Spark Ignition in an IC Gasoline Automotive Engine: a Comparative Study, SAE Technical Paper, 2008, 2008-01-0470.
- [23] J. Tauer, H. Kofler, E. Wintner, Laser-initiated ignition, *Laser Photon. Rev.* 4 (1) (2010) 99–122.
- [24] M.H. Morsy, Review and recent developments of laser ignition for internal combustion engines applications, *Renew. Sustain. Energy Rev.* 16 (7) (2012) 4849–4875.
- [25] A. Stakhiv, R. Gilber, H. Kopecek, A.M. Zheltikov, E. Wintner, Laser ignition of engines via optical fibers, *Laser Phys.* 14 (5) (2004) 738–747.
- [26] A.P. Yalin, M. DeFoort, B. Willson, Y. Matsuura, M. Miyagi, Use of hollow-core fibers to deliver nanosecond Nd:YAG laser pulses to form sparks in gases, *Opt. Lett.* 30 (16) (2005) 2083–2085.
- [27] A.H. Al-Janabi, Transportation of nanosecond laser pulses by hollow core photonic crystal fiber for laser ignition, *Laser Phys. Lett.* 2 (11) (2005) 529–531.
- [28] S. Joshi, A.P. Yalin, A. Galvanauskas, Use of hollow core fibers, fiber lasers, and photonic crystal fibers for spark delivery and laser ignition in gases, *Appl. Optics* 46 (19) (2007) 4057–4064.
- [29] H. El-Rabii, G. Gaborel, Laser ignition of flammable mixtures via a solid core optical fiber, *Appl. Phys. B-Lasers Opt.* 87 (1) (2007) 139–144.
- [30] D. Mullett, G. Dearden, R. Dodd, A.T. Shenton, G. Triantos, K.G. Watkins, A comparative study of optical fiber types for application in a laser-induced ignition system, *J. Opt. A-Pure Appl. Opt.* 11 (5) (2009) art. 054007.
- [31] S. Joshi, N. Wilvert, A.P. Yalin, Delivery of high intensity beams with large clad step-index fibers for engine ignition, *Appl. Phys. B-Lasers Opt.* 108 (4) (2012) 925–932.
- [32] A.P. Yalin, High power fiber delivery for laser ignition applications, *Opt. Express* 21 (S6) (2013) A1102–A1112.
- [33] G. Dearden, T. Shenton, Laser ignited engines: progress, challenges and prospects, *Opt. Express* 21 (S6) (2013) A1113–A1125.
- [34] C. Dumitrache, J. Rath, A. Yalin, High power spark delivery system using hollow core Kagome lattice fibers, *Materials* 7 (8) (2014) 5700–5710.
- [35] M. Weinrotter, H. Kopecek, E. Wintner, Laser ignition of engines, *Laser Phys.* 15 (7) (2005) 947–953.
- [36] Martin Weinrotter, Laser Ignition of Internal Combustion Engines: Basic Laser and Ignition Optics Developments, Engine Application and Optical Diagnostics, GRIN Verlag, 31-Mar-2011.
- [37] H. Kofler, J. Tauer, G. Tartar, K. Iskra, J. Klausner, G. Herdin, E. Wintner, An innovative solid-state laser for engine ignition, *Laser Phys. Lett.* 4 (4) (2007) 322–327.
- [38] E. Schwarz, I. Muri, J. Tauer, H. Kofler, E. Wintner, Laser-induced ignition by optical breakdown, *Laser Phys.* 20 (6) (2010) 1545–1553.

- [39] N. Pavel, J. Saikawa, S. Kurimura, T. Taira, High average power diode end-pumped composite Nd:YAG laser passively Q-switched by Cr⁴⁺:YAG saturable absorber, *Jpn. J. Appl. Phys.* 40 (Part 1, No. 3A) (2001) 1253–1259.
- [40] T. Taira, Y. Matsuoka, H. Sakai, A. Sone, H. Kan, Passively Q-switched Nd:YAG microchip laser over 1-MW peak output power for micro drilling, in: Conference on Lasers and Electro-optics/quantum Electronics and Laser Science Conference and Photonic Applications Systems Technologies, Technical Digest (CD), Optical Society of America, 2006 paper CWF6.
- [41] M. Tsunekane, T. Inohara, A. Ando, K. Kanehara, T. Taira, High peak power, passively Q-switched Cr:YAG/Nd:YAG micro-laser for ignition of engines, in: Advanced Solid-state Photonics, OSA Technical Digest Series (CD), Optical Society of America, 2008 paper MB4.
- [42] H. Sakai, H. Kan, T. Taira, >1 MW peak power single-mode high-brightness passively Q-switched Nd³⁺: YAG microchip laser, *Opt. Express* 16 (24) (2008) 19891–19899.
- [43] M. Tsunekane, T. Inohara, A. Ando, N. Kido, K. Kanehara, T. Taira, High peak power, passively Q-switched microlaser for ignition of engines, *IEEE J. Quantum Electron.* 46 (2) (2010) 277–284.
- [44] M. Tsunekane, T. Inohara, K. Kanehara, T. Taira, Micro-solid-state laser for ignition of automobile engines, in: M. Grishin (Ed.), *Advances in Solid State Lasers - Development and Applications*, 2010. InTech.
- [45] N. Pavel, M. Tsunekane, K. Kanehara, T. Taira, Composite all-ceramics, passively q-switched Nd:YAG/Cr⁴⁺:YAG monolithic micro-laser with two-beam output for multi-point ignition, in: CLEO: 2011-Laser Applications to Photonic Applications, OSA Technical Digest (CD), Optical Society of America, 2011 paper CMP1.
- [46] N. Pavel, M. Tsunekane, T. Taira, Composite, all-ceramics, high-peak power Nd:YAG/Cr⁴⁺:YAG monolithic micro-laser with multiple-beam output for engine ignition, *Opt. Express* 19 (10) (2011) 9378–9384.
- [47] N. Pavel, M. Tsunekane, T. Taira, All-poly-crystalline ceramics Nd:YAG/Cr⁴⁺:YAG monolithic micro-lasers with multiple-beam output, in: Dr Krzysztof Jakubczak (Ed.), *Laser Systems for Applications*, 2011. InTech.
- [48] M. Tsunekane, T. Taira, High peak power, passively Q-switched Yb:YAG/Cr:YAG micro-lasers, *IEEE J. Quantum Electron.* 49 (5) (2013) 454–461.
- [49] M. Tsunekane, T. Taira, Yb:YAG/Cr:YAG passively Q-switched microlaser for ignition, in: 1st Laser Ignition Conference, Yokohama, Japan, 2013 paper LIC4–4.
- [50] M. Tsunekane, T. Taira, Thin rod micro-laser for ignition, in: 2nd Laser Ignition Conference, Yokohama, Japan, 2014 paper LIC9–2.
- [51] M. Tsunekane, T. Taira, Long time operation of composite ceramic Nd:YAG/Cr:YAG micro-chip lasers for ignition, in: Laser Ignition Conference, OSA Technical Digest (Online), Optical Society of America, 2015 paper T4A.3.
- [52] T. Taira, S. Morishima, K. Kanehara, N. Taguchi, A. Sugiura, M. Tsunekane, World first laser ignited gasoline engine vehicle, in: 1st Laser Ignition Conference, Yokohama, Japan, 2013 paper LIC3–1.
- [53] G. Kroupa, G. Franz, E. Winkelhofer, Novel miniaturized high-energy Nd:YAG laser for spark ignition in internal combustion engines, *Opt. Eng.* 48 (1) (2009) art. 014202.
- [54] G. Kroupa, M. Baumgart, A. Tortschanoff, A highly robust, miniaturized Nd:YAG laser for spark ignition, in: 1st Laser Ignition Conference, Yokohama, Japan, 2013 paper LIC5–4.
- [55] C. Manfletti, G. Kroupa, Laser ignition of a cryogenic thruster using a miniaturised Nd:YAG laser, *Opt. Express* 21 (S6) (2013) A1126–A1139.
- [56] G. Kroupa, G. Bruckner, N. Rackemann, S. Soller, Laser ignition for aerospace applications using the rugged miniaturized HiPoLas[®] Nd:YAG laser system, in: Laser Ignition Conference 2017, OSA Technical Digest (Online), Optical Society of America, 2017 paper LThA4.1.
- [57] Y. Ma, X. Li, X. Yu, R. Fan, R. Yan, J. Peng, X. Xu, R. Sun, D. Chen, A novel miniaturized passively Q-switched pulse-burst laser for engine ignition, *Opt. Express* 22 (20) (2014) 24655–24665.
- [58] P. Wörner, H. Ridderbusch, J. Ostrinsky, U. Meingast, History of laser ignition for large gas engines at Robert Bosch GmbH, in: 2nd Laser Ignition Conference, Yokohama, Japan, 2014 paper LIC3–2.
- [59] J. Schwarz, K. Stoppel, K.-H. Nübel, J. Engelhardt, Pumping concepts for laser spark plugs - requirements, options, solutions, in: 2nd Laser Ignition Conference, Yokohama, Japan, 2014 paper LIC3–3.
- [60] R. Hartke and K. H. Nuebel, Laser Spark Plug for an Internal Combustion Engine, and Production Method Herefor, WO 2012069228 A3 PCT/EP2011/066411.
- [61] T. Dascalu, N. Pavel, High-temperature operation of a diode-pumped passively Q-switched Nd: YAG/Cr⁴⁺:YAG laser, *Laser Phys.* 19 (11) (2009) 2090–2095.
- [62] N. Pavel, M. Tsunekane, T. Taira, Enhancing performances of a passively Q-switched Nd:YAG/Cr⁴⁺:YAG microlaser with a volume Bragg grating output coupler, *Opt. Lett.* 35 (10) (2010) 1617–1619.
- [63] G. Salamu, O. Sandu, F. Voicu, M. Dejanu, D. Popa, S. Parlac, C. Ticos, N. Pavel, T. Dascalu, Study of flame development in 12% methane-air mixture ignited by laser, *Optoelectron. Adv. Mater.-Rapid Commun.* 5 (11) (2011) 1166–1169.
- [64] T. Dascalu, G. Salamu, O. Sandu, F. Voicu, N. Pavel, Novel laterally pumped by prism laser configuration for compact solid-state lasers, *Laser Phys. Lett.* 10 (5) (2013) art. 055804.
- [65] N. Pavel, G. Salamu, T. Dascalu, Passively Q-switched, composite Nd:YAG/Cr⁴⁺:YAG laser pumped laterally through a prism, in: 2nd Laser Ignition Conference, Yokohama, Japan, 2014 paper LIC5–2.
- [66] T. Dascalu, G. Salamu, O. Sandu, M. Dinca, N. Pavel, Scaling and passively Q-switch operation of a Nd:YAG laser pumped laterally through a YAG prism, *Opt. Laser Technol.* 67 (2015) 164–168.
- [67] N. Pavel, T. Dascalu, G. Salamu, M. Dinca, N. Boicea, A. Birtas, Ignition of an automobile engine by high-peak power Nd:YAG/Cr⁴⁺:YAG laser-spark devices, *Opt. Express* 23 (26) (2015) 33028–33037.
- [68] J. Shirley, Engine Window Soot Removal by a Laser Shock Cleaning Process, MSc(Eng) Thesis, Department of Engineering, University of Liverpool, 2003.
- [69] H. Ranner, P.K. Tewari, H. Koefler, M. Lackner, E. Wintner, A.K. Agarwal, F. Wintner, Laser cleaning of optical windows in internal combustion engines, *Opt. Eng.* 46 (10) (2007) art. 104301.
- [70] A. Birtas, G. Croitoru (Salamu), M. Dinca, T. Dascalu, N. Boicea, N. Pavel, The effect of laser ignition on a homogenous lean mixture of an automotive gasoline engine, in: 4th Laser Ignition Conference, Yokohama, Japan, 2016 paper LIC6–2.
- [71] A. Birtas, N. Boicea, G. Croitoru, M. Dinca, T. Dascalu, N. Pavel, Combustion characteristics of a gasoline-air mixture laser ignition, in: Laser Ignition Conference 2017, OSA Technical Digest (Online), Optical Society of America, 2017 paper LFA3.4.
- [72] N. Pavel, A. Birtas, G. Croitoru, M. Dinca, N. Boicea, T. Dascalu, Laser ignition of a gasoline engine automobile, in: Laser Ignition Conference 2017, OSA Technical Digest (Online), Optical Society of America, 2017 paper LWA4.3.
- [73] L. Goldberg, C. McIntosh, B. Cole, VCSEL end-pumped passively Q-switched Nd:YAG laser with adjustable pulse energy, *Opt. Express* 19 (5) (2011) 4261–4267.
- [74] Y. Xiong, R. Van Leeuwen, L.S. Watkins, J.-F. Seurin, G. Xu, A. Miglo, Q. Wang, C. Ghosh, High power VCSEL array pumped Q-switched Nd:YAG lasers, in: *Solid State Lasers XXI: Technology and Devices Proc. SPIE* 8235, 2012, 82350M.
- [75] E. Wintner, Implications of ambient temperature on a laser spark plug, in: 1st Laser Ignition Conference, Yokohama, Japan, 2013 paper LIC2–1.
- [76] M. Tsunekane, T. Taira, Ignition lasers operating for wide temperature range, in: 1st Laser Ignition Conference, Yokohama, Japan, 2013 paper LIC2–3.
- [77] S. Gronenborn, R. Conrads, M. Miller, H. Moench, P. Pekarski, J. Pollman-Retsch, A. Pruijboom, J. Pankert, VCSEL power arrays as ideal pump source for laser ignition, in: 2nd Laser Ignition Conference, Yokohama, Japan, 2014 paper LIC7–2.
- [78] T. Suzudo, K. Hagita, T. Ikeo, K. Izumiya, N. Jikutani, Y. Higashi, T. Taira, Total design of high power VCSEL pumped passively Q-switched micro-lasers for laser ignition, in: 4th Laser Ignition Conference, Yokohama, Japan, 2016 paper LIC3–1.
- [79] K. Hagita, T. Ikeo, Y. Ishikawa, Y. Higashi, N. Jikutani, T. Taira, T. Suzudo, Multi-pulse oscillation of passively Q-switched micro-laser pumped by VCSEL module, in: 4th Laser Ignition Conference, Yokohama, Japan, 2016 paper LIC3–2.
- [80] K. Izumiya, Y. Ohkura, M. Numata, N. Arai, K. Ikeda, Y. Sasaki, N. Jikutani, T. Suzudo, 808 nm range high-power (QCW 200 W) fiber-coupled VCSEL module for laser ignition, in: 4th Laser Ignition Conference, Yokohama, Japan, 2016 paper LIC3–4.
- [81] T. Ikeo, K. Hagita, Y. Ishikawa, Y. Higashi, N. Jikutani, T. Taira, T. Suzudo, Improvement the optical-to-optical conversion efficiency of passively Q-switched micro-laser pumped by VCSEL module, in: Laser Ignition Conference 2017, OSA Technical Digest (Online), Optical Society of America, 2017 paper LWA2.2.
- [82] Princeton Optronics, High Power VCSEL Laser Igniter. [Online] Available: <http://www.princetonoptronics.com/product/high-power-vcsel-laser-igniter/>.

- [83] T. Phuoc, Single-point versus multi-point laser ignition: experimental measurements of combustion times and pressures, *Combust. Flame* 122 (4) (2000) 508–510.
- [84] M.H. Morsy, Y.S. Ko, S.H. Chung, Laser-induced ignition using a conical cavity in CH₄-air mixtures, *Combust. Flame* 119 (4) (1999) 473–482.
- [85] M.H. Morsy, Y.S. Ko, S.H. Chung, P. Cho, Laser-induced two-point ignition of premixture with a single-shot laser, *Combust. Flame* 124 (4) (2001) 724–727.
- [86] M.H. Morsy, S.H. Chung, Laser-induced multi-point ignition with a single-shot laser using two conical cavities for hydrogen/air mixture, *Exp. Therm. Fluid Sci.* 27 (4) (2003) 491–497.
- [87] S.H. Chung, Laser-induced multi-point ignition for enabling high-performance engines, in: *Laser Ignition Conference*, OSA Technical Digest (Online), Optical Society of America, 2015 paper W2A.7.
- [88] K. Horie, S. Sato, S. Nakaya, M. Tsue, Ignition behaviour of lean methane/air mixture by close dual-point laser-induced sparks, in: *1st Laser Ignition Conference*, Yokohama, Japan, 2013 paper LIC7–2.
- [89] S. Yamaguchi, E. Takahashi, H. Furutani, H. Kojima, S. Inami, J. Miyata, T. Kashiwazaki, M. Nishioka, Two-point laser ignition for stable lean burn operation of gas engine, in: *2nd Laser Ignition Conference*, Yokohama, Japan, 2014 paper LIC8–4.
- [90] T. Saito, Y. Suzuta, E. Takahashi, H. Furutani, Performance of internal combustion engine using multi-point laser ignition under nitrogen dilution conditions, in: *4th Laser Ignition Conference*, Yokohama, Japan, 2016 paper LIC6–5.
- [91] T. Saito, T. Sugaya, E. Takahashi, H. Furutani, Influence of laser incident energy and focal length on multi-point laser ignition in an internal combustion engine at N₂ dilution, in: *Laser Ignition Conference 2017*, OSA Technical Digest (Online), Optical Society of America, 2017 paper LWA4.2.
- [92] R. Grzeszlik, Impact of turbulent in-cylinder air motion and local mixture formation on inflammation in lean engine operation: is multiple point ignition a solution?, in: *Laser Ignition Conference 2017*, OSA Technical Digest (Online) Optical Society of America, 2017 paper LFA3.1.
- [93] Y. Ma, Y. He, X. Yu, X. Li, J. Li, R. Yan, J. Peng, X. Zhang, R. Sun, Y. Pan, D. Chen, Multiple-beam, pulse-burst, passively Q-switched ceramic Nd:YAG laser under micro-lens array pumping, *Opt. Express* 23 (19) (2015) 24955–24961.
- [94] T. Dascaľu, G. Croitoru, O. Grigore, N. Pavel, High-peak-power passively Q-switched Nd: YAG/Cr⁴⁺:YAG composite laser with multiple-beam output, *Photonics Res.* 4 (6) (2016) 267–271.
- [95] E. Lyon, Z. Kuang, H. Cheng, V. Page, A.T. Shenton, G. Dearden, Multi-point laser spark generation for internal combustion engines using a spatial light modulator, *J. Phys. D-Appl. Phys.* 47 (47) (2014) art. 475501.
- [96] G. Dearden, Z. Kuang, E. Lyon, H. Cheng, V. Page, T. Shenton, Multi-point laser ignition for in-combustion event feedback control of an automobile engine, in: *4th Laser Ignition Conference*, Yokohama, Japan, 2016 paper LIC6–1.
- [97] Z. Kuang, E. Lyon, H. Cheng, V. Page, T. Shenton, G. Dearden, Multi-location laser ignition using a spatial light modulator towards improving automotive gasoline engine performance, *Opt. Lasers Eng.* 90 (2017) 275–283.
- [98] H. Kojima, E. Takahashi, H. Furutani, Laser ignition controlled by the combination of nano- and femto-second lasers, in: *1st Laser Ignition Conference*, Yokohama, Japan, 2013 paper LIC7–3.
- [99] H. Kojima, E. Takahashi, H. Furutani, Breakdown plasma and vortex flow control for laser ignition using a combination of nano- and femto-second lasers, *Opt. Express* 22 (1) (2014) A90–A98.
- [100] N. Beheran, R. George, M. Orain, L. Zimmer, Optimising double-pulse strategy for spray ignition, in: *4th Laser Ignition Conference*, Yokohama, Japan, 2016 paper LIC2–2.
- [101] S. Lorenz, M. Bärwinkel, R. Stäglich, W. Mühlbauer, D. Brüggemann, Pulse train ignition with passively Q-switched laser spark plugs, *Int. J. Engine Res.* 17 (1) (2016) 139–150.
- [102] P.S. Hsu, S. Roy, Z. Zhang, J. Sawyer, M.N. Slipchenko, J.G. Mance, J.R. Gord, High-repetition-rate laser ignition of fuel-air mixtures, *Opt. Lett.* 41 (7) (2016) 1570–1573.
- [103] J.D. Mullett, R. Dodd, C.J. Williams, G. Triantos, G. Dearden, A.T. Shenton, K.G. Watkins, S.D. Carroll, A.D. Scarisbrick, S. Keen, The influence of beam energy, mode and focal length on the control of laser ignition in an internal combustion engine, *J. Phys. D-Appl. Phys.* 40 (15) (2007) 4730–4739.
- [104] D.K. Srivastava, E. Wintner, A.K. Agarwal, Effect of focal size on the laser ignition of compressed natural gas-air mixture, *Opt. Lasers Eng.* 58 (2014) 67–79.
- [105] D.K. Srivastava, E. Wintner, A.K. Agarwal, Effect of laser pulse energy on the laser ignition of compressed natural gas fueled engine, *Opt. Eng.* 53 (5) (2014) art. 56120.
- [106] S. Lorenz, M. Bärwinkel, P. Heinz, S. Lehmann, W. Mühlbauer, D. Brüggemann, Characterization of energy transfer for passively Q-switched laser ignition, *Opt. Express* 23 (3) (2015) 2647–2659.
- [107] M. Bärwinkel, S. Lorenz, R. Stäglich, D. Brüggemann, Influence of focal point properties on energy transfer and plasma evolution during laser ignition process with a passively q-switched laser, *Opt. Express* 24 (14) (2016) 15189–15203.
- [108] D.L. McIntyre, *Laser Spark Plug Ignition System for a Stationary Lean-burn Natural Gas Reciprocating Engine*, Ph.D. Dissertation, West Virginia University, 2007.
- [109] D.L. McIntyre, S.D. Woodruff, M.H. McMillian, S.W. Richardson, M. Gautam, Laser Spark Plug Development, SAE Technical Paper, 2007, 2007-01-1600.
- [110] D.L. McIntyre, S.D. Woodruff, J.S. Ontko, Lean-burn stationary natural gas engine operation with a prototype laser spark plug, *J. Eng. Gas Turbines Power* 132 (7) (2010) art. 072804.
- [111] S.B. Gupta, B. Bihari, M. Biruduganti, R. Sekar, Laser ignition in natural gas engine, in: *1st Laser Ignition Conference*, Yokohama, Japan, 2013 paper LIC9–1.
- [112] S.B. Gupta, B. Bihari, R. Sekar, Performance of a 6-cylinder natural gas engine on laser ignition, in: *2nd Laser Ignition Conference*, Yokohama, Japan, 2014 paper LIC6–3.
- [113] M. Biruduganti, S. Gupta, B. Bihari, K. Kanehara, N. Polcyn, J. Hwang, Performance evaluation of a DENSO developed micro-laser ignition system on a natural gas research engine, in: *Laser Ignition Conference*, OSA Technical Digest (Online), Optical Society of America, 2015 paper T5A.4.
- [114] B. Bihari, M. Biruduganti, S. Gupta, Natural gas engine performance ignited by a passively Q-Switched microlaser, in: *Laser Ignition Conference*, OSA Technical Digest (Online), Optical Society of America, 2015 paper T5A.5.
- [115] S. Gupta, B. Bihari, M. Biruduganti, Q. Wang, R. Van Leeuwen, Performance benefits of laser ignition in a natural gas 6-cylinder engine, in: *4th Laser Ignition Conference*, Yokohama, Japan, 2016 paper LIC8–2.
- [116] B. Almansour, S. Vasu, Q. Wang, R. Van Leeuwen, S. Gupta, B. Bihari, Performance of laser and spark ignition systems in a reciprocating natural gas engine, in: *Laser Ignition Conference 2017*, OSA Technical Digest (Online), Optical Society of America, 2017 paper LThA3.1.
- [117] H. Koizumi, T. Hayashi, K. Komurasaki, Diode laser ignition of solid propellants for small satellite propulsion system, in: *2nd Laser Ignition Conference*, Yokohama, Japan, 2014 paper LIC4–4.
- [118] C. Manfletti, M. Börner, Laser ignition for space propulsion systems, in: *Laser Ignition Conference*, OSA Technical Digest (Online), Optical Society of America, 2015 paper Th2A.3.
- [119] C. Manfletti, M. Börner, Future space transportation, propulsion systems and laser ignition, in: *Laser Ignition Conference 2017*, OSA Technical Digest (Online), Optical Society of America, 2017 paper LFA4.1.
- [120] M. Börner, J.C. Deeken, C. Manfletti, M. Oschwald, Determination of the minimum laser pulse energies for ignition in a subscale rocket combustion chamber, in: *Laser Ignition Conference 2017*, OSA Technical Digest (Online), Optical Society of America, 2017 paper LThA4.2.
- [121] J. Griffiths, A. Kirk, C. Dowding, Minimum operation requirements for laser ignition in gas turbines, in: *4th Laser Ignition Conference*, Yokohama, Japan, 2016 paper LIC8–4.
- [122] G. Amiard-Hudebine, G. Tison, E. Freysz, Compact nanosecond laser system for the ignition of aeronautic combustion engines, *J. Appl. Phys.* 120 (23) (2016) art. 233102.
- [123] S.A. O'Briant, S.B. Gupta, S.S. Vasu, Review: laser ignition for aerospace propulsion, *Propuls. Power Res.* 5 (1) (2016) 1–21.
- [124] D. Srivastava, A.K. Agarwal, Laser Ignition of Single Cylinder Engine and Effects of Ignition Location, SAE Technical Paper, 2013, 2013-01-1631.
- [125] D.K. Srivastava, A.K. Agarwal, Comparative experimental evaluation of performance, combustion and emissions of laser ignition with conventional spark plug in a compressed natural gas fuelled single cylinder engine, *Fuel* 123 (2014) 113–122.

- [126] S. Yamaguchi, T. Kashiwazaki, M. Nishioka, E. Takahashi, H. Furutani, H. Kojima, J. Miyata, Dual-point laser ignition and its location effects on combustion in lean-burn gas engine, *SAE Int. J. Engines* 8 (3) (2015) 1435–1446.
- [127] H. Cheng, Z. Kuang, V. Page, E. Lyon, G. Dearden, T. Shenton, Multiple pulse laser ignition in GDI lean combustion, *Int. J. Powertrains* 5 (1) (2016) 55–68.
- [128] L.J. Radziemski, D.A. Cremers, *Laser-induced Plasmas and Applications*, M. Dekker, New York, 1989.
- [129] E. Yablonoitch, Self-phase modulation and short-pulse generation from laser-breakdown plasmas, *Phys. Rev. A* 10 (5) (1974) 1888–1895.
- [130] Y.P. Raizer, Breakdown and heating of gases under the influence of a laser beam, *Sov. Phys. Usp.* 8 (5) (1966) 650–673.
- [131] Y.P. Raizer, Heating of a gas by a powerful light pulse, *J. Exp. Theor. Phys.* 21 (5) (1965) 1009–1017.
- [132] T.X. Phuoc, Laser spark ignition: experimental determination of laser-induced breakdown thresholds of combustion gases, *Opt. Commun.* 175 (4–6) (2000) 419–423.
- [133] S.S. Harilal, B.E. Brumfield, M.C. Phillips, Lifecycle of laser-produced air sparks, *Phys. Plasmas* 22 (6) (2015) art. 063301.
- [134] P. Gregorič, J. Diaci, J. Možina, Two-dimensional measurements of laser-induced breakdown in air by high-speed two-frame shadowgraphy, *Appl. Phys. A-Mater. Sci. Process.* 112 (1) (2013) 49–55.
- [135] C. Leela, S. Bagchi, V.R. Kumar, S.P. Tewari, P.P. Kiran, Dynamics of laser induced micro-shock waves and hot core plasma in quiescent air, *Laser Part. Beams* 31 (2) (2013) 263–272.
- [136] Y.-L. Chen, J.W.L. Lewis, Visualization of laser-induced breakdown and ignition, *Opt. Express* 9 (7) (2001) 360–372.
- [137] H. El-Rabii, J.C. Rolon, Experimental study of laser ignition of a methane/air mixture by planar laser-induced fluorescence of OH, in: *Proceedings of PSFVIP4, Chamonix Mont-blanc, Frankreich, 2003. F4022*.
- [138] M. Lackner, S. Charareh, F. Winter, K.F. Iskra, D. Rüdiger, T. Neger, H. Kopecek, E. Wintner, Investigation of the early stages in laser-induced ignition by Schlieren photography and laser-induced fluorescence spectroscopy, *Opt. Express* 12 (19) (2004) 4546–4557.
- [139] Y.-L. Chen, J.W.L. Lewis, C. Parigger, Spatial and temporal profiles of pulsed laser-induced air plasma emissions, *J. Quant. Spectrosc. Radiat. Transf.* 67 (2) (2000) 91–103.
- [140] S. Brieschenk, H. Kleine, S. O'Byrne, On the measurement of laser-induced plasma breakdown thresholds, *J. Appl. Phys.* 114 (9) (2013) art. 093101.
- [141] J.L. Beduneau, N. Kawahara, T. Nakayama, E. Tomita, Y. Ikeda, Laser-induced radical generation and evolution to a self-sustaining flame, *Combust. Flame* 156 (3) (2009) 642–656.
- [142] M.S. Bak, L. Wermer, S.-k. Im, Schlieren imaging investigation of successive laser-induced breakdowns in atmospheric-pressure air, *J. Phys. D-Appl. Phys.* 48 (48) (2015) art. 485203.
- [143] M.S. Bak, S.-k. Im, M.A. Cappelli, Successive laser-induced breakdowns in atmospheric pressure air and premixed ethane–air mixtures, *Combust. Flame* 161 (7) (2014) 1744–1751.
- [144] E. Schwarz, S. Gross, B. Fischer, I. Muri, J. Tauer, H. Kofler, E. Wintner, Laser-induced optical breakdown applied for laser spark ignition, *Laser Part. Beams* 28 (1) (2010) 109–119.
- [145] C. Cardin, B. Renou, G. Cabot, A.M. Boukhalfa, Experimental analysis of laser-induced spark ignition of lean turbulent premixed flames: new insight into ignition transition, *Combust. Flame* 160 (8) (2013) 1414–1427.
- [146] X. Li, B.W. Smith, N. Omenetto, Laser spark ignition of premixed methane-air mixtures: parameter measurements and determination of key factors for ultimate ignition results, *Appl. Spectrosc.* 68 (9) (2014) 975–991.
- [147] C.V. Bindhu, S.S. Harilal, M.S. Tillack, F. Najmabadi, A.C. Gaeris, Laser propagation and energy absorption by an argon spark, *J. Appl. Phys.* 94 (12) (2003) 7402–7407.
- [148] J. Zabkar, M. Marincek, M. Zgonik, Mode competition during the pulse formation in passively Q-switched Nd:YAG lasers, *IEEE J. Quantum Electron.* 44 (4) (2008) 312–318.
- [149] J.M. Hendron, C.M.O. Mahony, T. Morrow, W.G. Graham, Langmuir probe measurements of plasma parameters in the late stages of a laser ablated plume, *J. Appl. Phys.* 81 (5) (1997) 2131–2134.
- [150] K. Dzierżęga, A. Mendys, B. Pokrzywka, What can we learn about laser-induced plasmas from Thomson scattering experiments, *Spectrosc. Acta Pt. B-Atom Spectr.* 98 (2014) 76–86.
- [151] A. Mendys, K. Dzierżęga, M. Grabiec, S. Pellerin, B. Pokrzywka, G. Travaillé, B. Bousquet, Investigations of laser-induced plasma in argon by Thomson scattering, *Spectrosc. Acta Pt. B-Atom Spectr.* 66 (9–10) (2011) 691–697.
- [152] H. Sobral, M. Villagrán-Muniz, R. Navarro-González, A.C. Raga, Temporal evolution of the shock wave and hot core air in laser induced plasma, *Appl. Phys. Lett.* 77 (20) (2000) 3158–3160.
- [153] S.Y. Oh, C. Lim, S.Y. Ha, S. Nam, J. Han, Experimental study of laser-induced air plasma using a Nomarski interferometer, *Jpn. J. Appl. Phys.* 54 (7) (2015) art. 076101.
- [154] H. Zhang, J. Lu, Z. Shen, X. Ni, Investigation of 1.06 μm laser induced plasma in air using optical interferometry, *Opt. Commun.* 282 (9) (2009) 1720–1723.
- [155] G.R. Plateau, N.H. Matlis, C.G.R. Geddes, A.J. Gonsalves, S. Shiraishi, C. Lin, R.A. van Mourik, W.P. Leemans, Wavefront-sensor-based electron density measurements for laser-plasma accelerators, *Rev. Sci. Instrum.* 81 (3) (2010) art. 033108.
- [156] S. Zhang, X. Wang, M. He, Y. Jiang, B. Zhang, W. Hang, B. Huang, Laser-induced plasma temperature, *Spectrosc. Acta Pt. B-Atom Spectr.* 97 (2014) 13–33.
- [157] M. Thiyagarajan, J. Scharer, Experimental investigation of ultraviolet laser induced plasma density and temperature evolution in air, *J. Appl. Phys.* 104 (1) (2008) art. 013303.
- [158] N. Glumac, G. Elliott, M. Boguszko, Temporal and spatial evolution of a laser spark in air, *AIAA J.* 43 (9) (2005) 1984–1994.
- [159] N. Kawahara, J.L. Beduneau, T. Nakayama, E. Tomita, Y. Ikeda, Spatially, temporally, and spectrally resolved measurement of laser-induced plasma in air, *Appl. Phys. B-Lasers Opt.* 86 (4) (2007) 605–614.
- [160] N. Glumac, G. Elliott, The effect of ambient pressure on laser-induced plasmas in air, *Opt. Lasers Eng.* 45 (10) (2007) 27–35.
- [161] D. Böker, D. Brüggemann, Temperature measurements in a decaying laser-induced plasma in air at elevated pressures, *Spectrosc. Acta Pt. B-Atom Spectr.* 66 (1) (2011) 28–38.
- [162] S. George, R.K. Singh, V.P.N. Nampoori, A. Kumar, Fast imaging of the laser-blow-off plume driven shock wave: dependence on the mass and density of the ambient gas, *Phys. Lett. A* 377 (5) (2013) 391–398.
- [163] B. Pokrzywka, A. Mendys, K. Dzierżęga, M. Grabiec, S. Pellerin, Laser light scattering in a laser-induced argon plasma: investigations of the shock wave, *Spectrosc. Acta Pt. B-Atom Spectr.* 74–75 (2012) 24–30.
- [164] C.V. Bindhu, S.S. Harilal, M.S. Tillack, F. Najmabadi, A.C. Gaeris, Energy absorption and propagation in laser-created sparks, *Appl. Spectrosc.* 58 (6) (2004) 719–726.
- [165] J.-L. Beduneau, Y. Ikeda, Spatial characterization of laser-induced sparks in air, *J. Quant. Spectrosc. Radiat. Transf.* 84 (2) (2004) 123–139.
- [166] J.-L. Beduneau, Y. Ikeda, Application of laser ignition on laminar flame front investigation, *Exp. Fluids* 36 (1) (2004) 108–113.
- [167] L. Cadwell, L. Hüwel, Time-resolved emission spectroscopy in laser-generated argon plasmas-determination of Stark broadening parameters, *J. Quant. Spectrosc. Radiat. Transf.* 83 (3–4) (2004) 579–598.
- [168] S.S. Harilal, Spatial and temporal evolution of argon spark, *Appl. Optics* 43 (19) (2004) 3931–3937.
- [169] W. Lochte-Holtgreven, *Plasma Diagnostics*, Edited by W. Lochte-Holtgreven. Contributors: J. Richter [and Others], North-Holland Publishing Company, 1968.
- [170] S. Lorenz, D. Brüggemann, Designing the early flame kernel structure by the laser pulse profile, in: *4th Laser Ignition Conference, Yokohama, Japan, 2016 paper LIC8–3*.
- [171] M. Villagrán-Muniz, H. Sobral, R. Navarro-Gonzalez, Shock and thermal wave study of laser-induced plasmas in air by the probe beam deflection technique, *Meas. Sci. Technol.* 14 (5) (2003) 614–618.
- [172] B. Wang, K. Komurasaki, Y. Arakawa, Influence of ambient air pressure on the energy conversion of laser-breakdown induced blast waves, *J. Phys. D-Appl. Phys.* 46 (37) (2013) art. 375201.
- [173] M. Thiyagarajan, J.E. Scharer, Experimental investigation of 193-nm laser breakdown in air, *IEEE Trans. Plasma Sci.* 36 (5) (2008) 2512–2521.

- [174] H. Hirahara, M. Fujinami, M. Kawahashi, Velocity measurement of induced flow by a laser focusing shock wave, *J. Therm. Sci.* 15 (1) (2006) 48–53.
- [175] S. Brieschenk, S. O'Byrne, H. Kleine, Ignition characteristics of laser-ionized fuel injected into a hypersonic crossflow, *Combust. Flame* 161 (4) (2014) 1015–1025.
- [176] S. Brieschenk, R. Hruschka, S. O'Byrne, H. Kleine, High-speed time-resolved visualisation of laser-induced plasma explosions, in: 28th International Congress on High-speed Imaging and Photonics, in *Proc. SPIE* 7126, 2009, 71260N.
- [177] G.S. Settles, *Schlieren and Shadowgraph Techniques: Visualizing Phenomena in Transparent Media*, Springer, Berlin, New York, 2001.
- [178] D.K. Srivastava, K. Dharamshi, A.K. Agarwal, Flame kernel characterization of laser ignition of natural gas–air mixture in a constant volume combustion chamber, *Opt. Lasers Eng.* 49 (9–10) (2011) 1201–1209.
- [179] R.K. Prasad, S. Jain, G. Verma, A.K. Agarwal, Laser ignition and flame kernel characterization of HCNG in a constant volume combustion chamber, *Fuel* 190 (2017) 318–327.
- [180] S. Brieschenk, S. O'Byrne, H. Kleine, Visualization of jet development in laser-induced plasmas, *Opt. Lett.* 38 (5) (2013) 664–666.
- [181] D. Böker, D. Brüggemann, Advancing lean combustion of hydrogen–air mixtures by laser-induced spark ignition, *Int. J. Hydrog. Energy* 36 (22) (2011) 14759–14767.
- [182] M.S. Bak, M.A. Cappelli, Successive laser ablation ignition of premixed methane/air mixtures, *Opt. Express* 23 (11) (2015) A419–A427.
- [183] T.A. Spiglanin, A. McIlroy, E.W. Fournier, R.B. Cohen, J.A. Syage, Time-resolved imaging of flame kernels: laser spark ignition of $H_2/O_2/Ar$ mixtures, *Combust. Flame* 102 (3) (1995) 310–328.
- [184] I.A. Mulla, S.R. Chakravarthy, N. Swaminathan, R. Balachandran, Evolution of flame-kernel in laser-induced spark ignited mixtures: a parametric study, *Combust. Flame* 164 (2016) 303–318.
- [185] M. Longenecker, L. Hüwel, L. Cadwell, D. Nassif, Laser-generated spark morphology and temperature records from emission and Rayleigh scattering studies, *Appl. Optics* 42 (6) (2003) 990–996.
- [186] D. Nassif, L. Hüwel, Appearance of toroidal structure in dissipating laser-generated sparks, *J. Appl. Phys.* 87 (5) (2000) art. 2127.
- [187] M. Mansour, N. Peters, L.-U. Schrader, Experimental study of turbulent flame kernel propagation, *Exp. Therm. Fluid Sci.* 32 (7) (2008) 1396–1404.
- [188] M. Lehner, D. Mewes, U. Dinglreiter, R. Tauscher (Eds.), *Applied Optical Measurements*, Springer Verlag Berlin and Heidelberg GmbH Co KG, 1999.
- [189] A.C. Eckbreth, *Laser Diagnostics for Combustion Temperature and Species*, second ed., Gordon and Breach Publ, Amsterdam, 1996.
- [190] K. Kohse-Höinghaus, J.B. Jeffries, *Applied Combustion Diagnostics*, Taylor & Francis, New York, 2002.
- [191] R.B. Miles, W.R. Lempert, J.N. Forkey, Laser Rayleigh scattering, *Meas. Sci. Technol.* 12 (5) (2001) R33–R51.
- [192] D. Hoffman, K.-U. Münch, A. Leipertz, Two-dimensional temperature determination in sooting flames by filtered Rayleigh scattering, *Opt. Lett.* 21 (7) (1996) 525–527.